Many thanks to the reviewers for their valuable suggestions!

Review 1

Specific Comments (Section/ Line / Comment):

- / - / The code-to-code results of section 2 seem very valuable for other BEM and vortex methods to compare to. Can these results be shared publicly, e.g., through a website?

Results are available by emailing the corresponding author. This info has been added in the data availability section.

2.1 / - / A couple comments. The general capability of each model is less important than the specific models employed in the study; suggest focusing only on the specific models employed. Also, for the BEM and vortex methods, it would be useful to add a table comparing/contrasting which models are employed, as well as the time/space discretizations used. The various subsections are a bit mixed now.

A table with a high level overview is added.

2.3 / 209 / The text says shear is neglected from case Nr 1. Is that the same for all cases?

Yes this is the case and is now more explicitly stated in the paper.

2.3 / - / It would be useful to add a table comparing the computational expense, including real time and number of cores.

Yes this would be very useful but the info is not really available

2.3 / 216 / Were the rotor speed and pitch derived from one simulation and applied

to all simulation model, or just applied to the CFD? It would be preferred if they were

applied to all simulations.

From 1 simulation and applied to all models. This is clarified better in the text now.

2.4 / 368 / It would be useful to add a figure to clarify this approach of sector averaging.

Illustration is added to figure 7

3.2 / 413 / What is meant by "standard error the mean" when sigma contains the standard deviation?

The standard error of the mean within each bin is a measure for repeatability of the mean values collected within a bin. It is common practice in measurements to define it as equation 3 by dividing the standard deviation over the number of samples.

3.2 / 422 / Where the data provided by the manufacturer (especially aero) calibrated based on the field measurements?

No not as far as I am aware of. Reworded this sentence to clarify that blade data was delivered separately by the blade manufacturer.

3.2 / 425 / Was just the TI matched, or also the mean profile (shear), turbulence spectra,

spatial coherence, Reynolds stresses?

Only TI was matched. Sentence was added to clarify better.

4.1 / - / It would be also useful to mention thatgeometric details such as curvature, sweep, and/or deflection are also better captured by vortex methods over BEM.

Section 4.1 has been shortened

4.1 / - / This discussion is useful, but perhaps a bit out of place considering that no results are presented showing the differences between BEM and vortex methods for these load cases. Perhaps save this for a future publication where results will be presented?

Section 4.1 has been shortened

4.1 / 528 / DLC 6.X consider the turbine parked or idling, where the wake is expected to be minimal. Wouldn't a geometric AoA (without induction) suffice?

Section 4.1 has been rewritten

4.2 / 560 / The reviewer is unclear what is presented here. What is meant by "relative to the average..."?

A ratio is always relative to a certain number which in this case is the average over the two BEM simulations. Made a rewording attempt to better clarify this.

Technical Corrections (Section / Line / Comment):

1/ 17 / The first two sentences are a bit odd for an international journal. Suggest making more generic or discussing international growth.

Sentences replaced

2.1.4 / 153 / Add a space between "model" and "Snel".

ok

2.3.2 / -249 / Change "serie" to "series".

ok

2.3.3/ - / The data of Table 3 would be interpreted better as a bar chart.

Agree so modified

2.4 / 349 / The "W" in atan2 should be changed to "U".

Good spot!

2.4 / 353 / The reviewer's understanding is that these simulations considered a rigid structure,

so, there is no torsion deformation.

Indeed the cases featured in section 2.4 are rigid. The equations given however are intended for any general case.

3.2 / 409 / Clarify that "m=10".

Text modified

3.2 / 424 / Change "Turbsim" to "TurbSim".

ok

3.2 / - / Are the units on the legend purposely missing, e.g., to normalize the data?

Yes to comply with confidentiality (now indicated in the text)

Review 2

The paper presents a comparison of different classes of codes, evaluate differences in fatigue loads, suggests potential reasons for the differences observed, and present recommendations to use vortex wake models for some DLC loads cases. The study is thorough and convincing.

Here are my general comments:

- Shed vorticity is suggested as an explanation for the differences. Time constants of the dynamic stall and dynamic wake models are also likely to be a source of the "axial" induction filtering observed. I would actually think, the dynamic wake model might be the main source of error, since as you mentioned it is tuned to "cylindrical" wakes. You can investigate the effect of the time constants of these models on the axial induction to see if you can reach amplitudes similar to the ones observed for the vortex wake codes.

Indeed the dynamic wake model is also playing a role here, which was explained in section 2.2 in sheared inflow. The explanation has been expanded to section 2.3.2 as well to make the point more prominent.

- I would recommend to make a distinction between "vortex wake models" and "vortex methods" early on in the paper, or at least mention that what is meant by "vortex wake model" in the paper is low-order vortex filament methods. Vortex methods, in general, falls in the realm of CFD, and can be of the same order of accuracy as "traditional velocity-pressure CFD".

Clarification added in introduction

- I'm not sure I see the need to use the term "numerical wind tunnel", verification against "CFD simulations" seem more appropriate. It could be erroneously assumed that a "numerical wind tunnel" models walls, turbulence grid, etc.

Changed to CFD to prevent misinterpretation

- The presentation of the different codes are relevant and provide the appropriate details, yet I would recommend removing the mention of features that are not used in this study to avoid confusion. A table providing the differences in features (e.g. dynamic stall, high-thrust corrections, discretization, regularization parameters, viscous models, etc.) used by each code-class (BEM/Vortex) could be relevant as an introduction/conclusion of the second section.

A table with a high level overview is added

- Some of the figures can be improved for readability, and consistency (underscore are sometimes present, and units are not always present on the y-axis, but mentioned on the x axis). Since the study present differences between BEM and Vortex methods, it might be worth distinguishing between these two classes of codes in the figures. Even if a consistent color scheme has been used throughout the paper, having a way to clearly see which class of code is used would help the reader (with dashed lines or markers maybe). In general, I would think the explanations in the figure captions could be slightly extended.

Explanations in captions have been extended

- Last, I believe any attempt to shorten the length of the paper would be beneficial. I'll be happy to review a revised version of this manuscript.

Paper has been shortened slightly by restructuring section 4.1

Good luck for the remaining work,

Emmanuel

Here are my specific comments:

l78-84: Reporting the distances in diameter would be valuable.

Info added in table 1

l108: "dimensional form instead of nd factors": This is probably not as relevant as the

form of the equations itself, I don't think it's needed to mention this.

l121: The term Phatas is used in the text whereas PhatasSV is used in the figure.

Using one of the two terms throughout the document would avoid confusion.

Made consistent throughout the paper

l129-134: Since different features are listed here, it is not clear which ones will be used.

I'd recommend to only mention the ones that are used in this study and provide a link

to a documentation for more models.

All the ones mentioned here are used (dynamic stall and rotational effects excepted)

l140: Can you discuss the regularization/"viscous-core" model used for the bound circulation and for the wake: which model is used, how the regularization parameter is defined, does it include a "diffusion" model?

These parameters are typically important for wake studies (or wake interaction with a downstream rotor) but not really relevant for the loads studied in this project.

l145: Can you mention the typical number of filaments in the wake?

Info is added for the ECNAero-AWSM simulation. Because AWSM is also used when coupled to PhatAero, the order of these two code description sections has been swapped.

l159: Maybe "blade averaged induction" need to be reformulated since it seems to apply to the wake.

Reformulated

l250: It might not be obvious what "fixed" stands for (it's mentioned on the next line).

Order changed

l251-255: From figure 4a, it appears that the axial induction from vortex wake codes are significantly larger than the ones from the BEM codes. Can you expand your justification for the fatigue loads to be lower in this case? I would have expected the angle of attack fluctuations to be larger and the loads higher as well, but I might have missed something.

The variation in axial induced velocity is larger for vortex wake codes as it follows the inflow variations better. The resulting velocity triangle for a section will show the angle of attack to be more constant because the increase in wind is (partially) compensated by the increase in axial induction.

Figure 1: Could you provide the tangential force and C_T as well for all figures? The normal force is usually well captured. Depending on how these other component vary with the operating condition, it might not be necessary to show the radial distribution for the 4 wind speeds, 2 seem to be sufficient (at least looking at Fn).

Tangential force added for 2 velocities

Figure 1: Even if the axial induction is not present in CFD, it will be valuable to show this variable for the lifting-line codes since this is the core variable here (the rest of the angle of attack is purely defined by the free stream and the rotational speed).

As there is a good agreement in terms of forces as well as axial induction this variable is not shown here.

Figure 2: It would be relevant to show differences in mean as well as differences in amplitude.

The uniform inflow case was to establish agreement in terms of mean level, the sheared case focused on amplitudes. To reduce the nr of pages this information is left out here, but is available from the dedicated Vortexloads report.

Figure 4, 5: the caption should preferably mention what is meant by FIXED and BSV, BL_sector

Info is added

l299: "structural" might be confusing here.

Removed structural

l346: the tip-loss factor has also been ignored

Added in the sentence

l560: Could you mention some of the results from the tower loads?

Comment added

Reviewer 3

Dear authors,

this is a very interesting article on the validation of different aerodynamic codes for load calculations. Especially the comparison with field data is very impressive, and it is great how the reasons for differences between results from different codes are investigated in detail. However, there are some points where I don't quite understand what exactly is compared and how some of the models work. I am also suggesting a couple of references to Section 4 below, it's up to you if you want to include them.

Thank you for the good work! Please find my comments below.

General comments

* As a general comment there are many places in the article where \citep might be a better option than \cite.

Thanks for this great advice!

* An overview table of what kinds of corrections / models are used in the different BEM codes could be valuable.

Table with high level overview of codes was added

* It could be great if some of the data from the article could be shared. It would be very interesting for others to test their models in some of the cases and compare to your results as well as the CFD!

Results are available by emailing the corresponding author. This info has been added in the data availability section.

Specific comments

* Section 2.1.1 FLOWer: You write on line 95 that the airfoil data comes from CFD simulations. It's definitely a good idea to use 2D data on the outboard part for the vortex wake simulations. A few questions:

* Do you also use 2D data outside of 70% for the BEM simulations?

Yes

* Is it correctly understood that 3D polars have only been computed for the comparisons on the AVATAR turbine? So the comparison with measurements in Section 3 uses 'conventional' 2D airfoil data?

Yes

* Can you indicate at which AOA range you computed the CFD polars? And what did you do outside of that AOA range?

The 3D CFD polar data was extracted using the azimuthal averaged approach by varying the inflow speed while maintaining the rotational speed constant. This results in different polar range depending on the location of the airfoil section. In the inboard area, for example, the maximum angle can reach as large as 40 deg, while in the outer part it is smaller than that. As the main purpose for this dedicated approach is to correct the 3D effects in the root area of the blade, the extracted AoA range is sufficient. To cover for even larger AoA range, the original polar dataset of the AVATAR turbine was applied.

* As you write these polars include some 3D effects. Have you seen issues when using these polars up to 16 m/s with fairly high turbulence intensity? I would think these polars depend on the load distribution and at higher wind speeds the maximum loading and also the tip vortex will shift further inboard. Also the root vortex will become more important, so there may be an argument for

using 2D data closer to the root as well (If you have a root loss model in a BEM or when computing with AWSM).

Engineering model calculations employing the extracted 3D CFD polar perform very well in comparison to the fully resolved CFD data even for U = 25 m/s. This was demonstrated in a previous report (Page 18, Figures 17 and 18) [1], not only in terms of the integral loads but also in terms of the sectional loads. Root effects indeed strictly mean that 2D data needs to be used here as well but the project focus is not in this area.

[1] Bangga, Galih. "Comparison of blade element method and CFD simulations of a 10 MW wind turbine." Fluids 3, no. 4 (2018): 73.

References have been added

* Could the 3D CFD polars be made available?

Yes by emailing corresponding author who will redirect you to the responsible at Stuttgart Uni

* Section 2.1.2 Bladed 4.8

* Can you explain how the induced velocities are computed in Bladed? Is it an azimuth averaged approach? At least Figure 2 b) suggests that.

Section 2.2 explains this in more detail: "Application of the dynamic inflow model to the local element induced velocity (as implemented in the Bladed4.8-BEM results following the TUDK model as described in (Snel and Schepers, 1994)) appears to dampen out induced velocity variations in non-uniform inflow conditions"

* Section 2.1.3 Phatas

* I don't think I understand the purpose of the blade shed vorticity model in comparison with the 2D attached flow part of the Beddoes-Leishman dynamic stall model. It seems to me that

* Both model only the effect of the blade sections on themselves

* Both model the effect of the shed vorticity only (due to the time derivative of the circulation) at each section

* The Beddoes-Leishman model is probably easier to implement and faster to compute.

* Maybe I am missing the point but what is the advantage of the BSV model over the Beddoes-leishman model? Is it that the BSV model takes the finite blade length into account towards the tip? I am not sure I understand that from the reference. If it is about the finite blade length I would expect it to predict a smaller effect than the BL model (which is 2D), but in Figure 5 the effect of the BSV model seems to be a bit larger instead.

Since they are 2 models simulating the same thing (one acts on force coefficients and the other on induced velocity) it is interesting to compare.

* I assume that the dynamic stall model is without the second order terms that cause force variations for constant inflow and AOA in stalled conditions based on the strouhal number, is that correct?

Yes (clarification added)

* Section 2.2 Constant uniform and sheared inflow

    * Figure 2 a) Why are no flower results shown here?

They are there in black but the legend did not indicate it (fixed now).

    * line 193, 'calculations were done for various conditions'. A short summary of these conditions would be helpful to understand where the results in Figure 3 come from.

Wind speed range was added

    * line 200, The trend looks quadratic to me.

Observation modified

* Section 2.3.1 Comparison methodology

    * It sounds very promising how you made sure that the turbulence in CFD and lifting line codes matches. Is it possible to show a plot of the wind speed comparisons mentioned in line 240 to see how good the agreement is?

To reduce the number of pages this plot is shown in the dedicated Vortexloads report which is referenced

* Section 2.3.3 Effect of load case variations

    * Table 3: Why not show the EQLs in the same way as the INT and compare all three codes to CFD?

As mentioned: ‘Although comparison of equivalent loads between CFD and lifting line codes is hindered by small differences in inflow conditions, a comparison between lifting line codes (BEM and vortex) in terms of fatigue loading is deemed useful in the last two columns of Table 3’

* Section 2.4 Improved induction tracking

    * line 299: Maybe 'fundamental difference' instead of 'structural difference'? I'm not quite sure.

Modified

    * line 303: I would also expect that there will not be a big shed vorticity effect in vertical shear, because the time constants of the shed vorticity are in the order of chord length/(2 relative velocity). This is much faster than the 1P variations due to shear for most of the blade.

    * Equation (1): I would prefer C_t and U_i instead of Ct and Ui

    * Equation (2): Maybe you could name these wind speeds 'U' differently to make it clear that you use a wind speed for example 'U_m' for the momentum equations on the left side and 'U_f' for the force on the ritght side. These could then also be used in the text making it easier to understand how exactly the sector approach works.

This good idea is adapted

    * Figure 6:

        * Are you using local values for Ct and a? I think it is very important to be as specific as possible here.

Extra line is added to clarify how Ct and a are calculated

* Can you add points for BEM close to the tip (as you have for AWSM on the right side)? I would expect that the tip correction would make it not fall on the line for the momentum equations, and that would be a good thing.

Because the tip correction is used in the definition of a, the tip values are still on the momentum line and not shown here.

* line 367: Is it correctly understood that you use the sector wind speed 1) on the left hand side of Equation (2) and 2) in the computation of the induced velocity in Equation (1)? I think this should be written clearly in the text (possibly by also using for example 'U_m' in Equation (1) as suggested above for Equation (2).

Suggestion adopted

* line 386: I am not sure I understand what you mean by subiterations to ensure convergence of the momentum equations to avoid a lag due to the dynamic inflow. I think what the dynamic inflow model is supposed to do is to introduce time lags so that there is no equilibrium between the local forces and the induced wind at each time step. The momentum equations will only be converged in steady state. In our grid BEM implementation each point in a pure shear case is constantly in a steady state, that is why the dynamic inflow model is not contributing. Would your subiterations change the behaviour of the model for instance in the case of a pitch step in uniform inflow?

I think the initial text was unclear in the sense that I donot mean convergence between forces and induced wind only, but convergence between forces, induced wind and the dynamic inflow term. In our case this is not guaranteed because we have the annulus averaged induction (Ui_b1+Ui_b2+Ui_b3)/3 as convergence criterium. The text is rephrased to make this more clear.

* Section 3.3 Comparison to simulations

* line 445: Are you doing something in your implementation to 'deactivate' the shed vorticity part in stalled flow? Otherwise some unphysical lags of the effective AOA behind the geometric AOA in stall might cause some increased load spikes. We have tried to deal with that in 'Pirrung, G., & Gaunaa, M. (2018). Dynamic stall model modifications to improve the modeling of vertical axis wind turbines. DTU Wind Energy E, No. 171'. Not sure if this is responsible for the overall smaller than expected load reduction though, just an idea.

No specific implementation is done for shed vorticity in stalled flow. Thanks for this suggestion.

* Section 4 Impact on IEC design load calculations

* I think in general it could be nice to add some references here. I completely agree that vortex codes could give improved results in all the conditions you list, but there has been quite some effort in improving BEM modeling so some of the shortcomings of BEM are probably not as severe as they used to be.

Section 4.1 has been rewritten

* Line 472

* Suggested references: Wei Yu's work on dynamic inflow, our BEM paper, the Mexnext III final report, your torque paper from 2016

* Line 480 on large yaw misalignment

* Maybe a reference to the final report of mexnext 3 that includes some yaw comparisons would make sense

* Line 485

* High wind speeds are also a prime example of spanwise circulation variation, where the loading on the disc is far from uniform and Prandtl tip loss doesn't apply.

* I think a reference to our near wake model work that is directly adressing the missing spanwise coupling in BEM codes might be relevant here

* Line 490

* I think a reference to the radial induction model in our BEM paper or to Aagaard Madsen, H., Bak, C., Døssing, M., Mikkelsen, R. F., & Øye, S. (2010). Validation and modification of the Blade Element Momentum theory based on comparisons with actuator disc simulations. Wind Energy, 13(4), 373-389. could be relevant here

* line 500

* Are you sure that the wake effects are small? I agree that the complete induction is small but I think the effects at the individual blades due to tip/root loss can be substantial.

* line 532

* Same as just above: The disk loading is low but there may still be strong vorticity trailed from the blades that locally changes AOA quite a bit. What is important is that it can change whether parts of the blade are in stall or attached flow, which changes the aerodynamic damping of for example edgewise vibrations in stand still. You might name specifically that vortex induced vibrations may occur in 6.2, which can't be predicted by BEM or vortex codes.

* line 558 is the phataero-BEM including beddoes-leishman dynamic stall?

No

Validation and accommodation of vortex wake codes for wind turbine design load calculations

Koen Boorsma[1], Florian Wenz[2], Koert Lindenburg[3], Mansoor Aman[4], and Menno Kloosterman[3]

[1]ECN part of TNO, Petten, The Netherlands
[2]IAG University of Stuttgart, Stuttgart, Germany
[3]LM Windpower, Heerhugowaard, The Netherlands
[4]DNV-GL, Bristol, United Kingdom

Correspondence: K. Boorsma (koen.boorsma@tno.nl)

Abstract. The computational effort for wind turbine design loads calculations is more extreme than it is for other applications (e.g. aerospace) which necessitates the use of efficient but low-fidelity models. Traditionally the Blade Element Momentum (BEM) method is used to resolve the rotor aerodynamics loads for this purpose, as this method is fast and robust. With the current trend of increasing rotor size, and consequently large and flexible blades, a need has risen for a more accurate prediction of rotor aerodynamics. Previous work has demonstrated large improvement potential in terms of fatigue load predictions using vortex wake models together with a manageable penalty in computational effort.

The present publication has contributed towards making vortex wake models ready for application to certification load calculations. The observed reduction in flapwise blade root moment fatigue loading using vortex wake models instead of the Blade Element Momentum (BEM) method from previous publications has been verified using ~~a 'numerical wind tunnel', i.e.~~ Computational Fluid Dynamics (CFD) simulations. A validation effort against a long term field measurement campaign featuring 2.5MW turbines has also confirmed the improved prediction of unsteady load characteristics by vortex wake models against BEM based models in terms of fatigue loading. New light has been shed on the cause for the observed differences and several model improvements have been developed, both to reduce the computational effort of vortex wake simulations and to make BEM models more accurate. Scoping analyses for an entire fatigue load set have revealed the overall fatigue reduction may be up to 5% for the AVATAR 10MW rotor using a vortex wake rather than a BEM based code.

1 Introduction

~~It is expected that from 2025 offshore wind in Germany can operate without subsidy. Also in the Netherlands tenders without subsidy are emerging. To meet this goal large and reliable wind turbines are needed. At that time the size of wind turbines will be in the range of 13-15MW~~Increasing the size of wind turbine rotors is an important wind energy engineering objective, especially for the offshore industry. To make the most out of the expensive support structure, larger rotors can harvest more energy but also are subject to increased loads making them heavier. To beat the underlying square cube law, rotor blades are becoming more slender and flexible, which together with the larger inflow variations over the rotor disk result in highly unsteady flow features. For a reliable wind turbine design, dependable aerodynamic models are needed to reduce the large uncertainty margins associated with modeling these. At this moment roughly three categories of aerodynamic models are available:

1. Blade Element Momentum (BEM) models
2. Vortex wake models
3. Computational Fluid Dynamics (CFD) models

In the industry, the Blade Element Momentum method is the workhorse for wind turbine certification load calculations. Operating in the atmospheric boundary layer, these design load calculations feature a large number of aerodynamic iterations to define a representative load envelope. This necessitates the use of efficient but low-fidelity models ~~Schepers (2012)~~ (Schepers, 2012). The development of more advanced codes like vortex wake models for wind turbine applications started in early 2000 ~~Belessis et al. (2001); van Garrel (2003)~~(Belessis et al., 2001; van Garrel, 2003). Vortex wake models give a more accurate description of the rotor wake aerodynamics, but are more computationally expensive. Nevertheless with increasing computational power, vortex wake models are posing a good alternative to BEM. The vortex wake models subjected in this research are all low-order vortex filament methods. As part of the EU-project AVATAR~~Schepers (2016)~~ (Schepers, 2016) a fatigue load comparison round was performed between various aero-elastic codes using BEM and vortex wake models. Calculations were done featuring the AVATAR 10MW rotor in turbulent inflow for a variety of time averaged wind speeds. Two partners independently of each other showed a reduction of roughly 15% of the blade out of plane fatigue equivalent moments when switching from a BEM to a vortex wake type model for the evaluation of rotor aerodynamics (keeping the other parameters such as the structural dynamic model the same). Besides that large differences were found in the implementation of the BEM models. More results are given in the dedicated AVATAR report ~~Boorsma et al. (2016a)~~(Boorsma et al., 2016a). Over the last decades several publications have researched the added benefit of vortex wake models over BEM based models ~~Hauptmann et al (2014); Gupta (2006); Boorsma et al. (2016b)~~ (Hauptmann et al, 2014; Gupta, 2006; Boorsma et al., 2016b) and more recently ~~Perez-Becker et al. (2019)~~(Perez-Becker et al., 2019). Some of these feature a validation against wind tunnel data, for which the inflow conditions and turbine are not always representative for design load calculations on a multi MW wind turbine. Others, such as the mentioned AVATAR report, feature a comparison between BEM and vortex wake models for more representative conditions, but lack a validation since experimental data for these conditions are not available. Although one would expect a higher fidelity model to be more accurate, a validation and verification of the outcome is required to confirm the measured load prediction reduction form vortex wake type codes. Within this mindset the TKI WoZ VortexLoads project ~~Boorsma et al. (2019c)~~ (Boorsma et al., 2019c) was started in which ECN.TNO, DNV-GL, LM Windpower and GE have co-operated towards evaluating and accommodating the application of vortex wake models to certification load calculations. A comparison against ~~a 'numerical wind tunnel' or~~ dedicated CFD simulations in turbulent inflow conditions is carried out and described in section 2. A validation against a large field measurement database, which comprises of long term measurements to reduce the uncertainty in inflow conditions between measurements and simulations, is given in section 3. Lastly section 4 describes the impact of running a production load set with a vortex wake rather than a BEM type code.

2 Verification against ~~'numerical wind tunnel'~~CFD simulations

CFD simulations are carried out to verify the differences in dynamic loading and the resultant fatigue equivalents between BEM and vortex wake codes. ~~Hereto a 'numerical' wind tunnel was set-up subjecting a~~ A rigid (or non-flexible) version of the AVATAR 10MW wind turbine model was subject of study, which originated from the AVATAR project ~~Schepers (2016)~~ (Schepers, 2016). The various codes used in the comparison round and their settings are described first. The first focus is at comparisons in uniform, constant inflow and vertically sheared inflow, after which several cases with turbulent inflow conditions are studied.

2.1 Code descriptions

2.1.1 FLOWer

A CFD reference solution using the AVATAR 10MW rotor was calculated with the process chain for simulations of wind turbines developed at the Institute of Aerodynamics and Gas Dynamics (IAG, USTUTT) in the last years, i.e. ~~Schulz et al. (2016)~~ (Schulz et al., 2016). The main part of the chain is the CFD code FLOWer, which is complemented by different pre- and post-processing tools. The CFD code FLOWer was developed by the German Aerospace Center (DLR) within the MEGAFLOW project ~~Kroll et al. (2000)~~ (Kroll et al., 2000) in the late 1990s. It is a compressible code and solves the three dimensional, Navier-Stokes equations in an integral form with several turbulence models. The numerical scheme is based on a finite-volume formulation for block-structured grids. For the spatial discretization, a second order central discretization with artificial damping, Jameson-Schmidt-Turkel (JST) ~~Jameson et al. (1981)~~ (Jameson et al., 1981) method, and the 5th order weighted essentially non-oscillatory scheme WENO ~~Jiang and Shu (1996)~~ (Jiang and Shu, 1996) are available. Time integration is accomplished by an explicit multi-stage scheme. Time accurate simulations use the dual time stepping method as implicit scheme. The pseudo time iterations can be accelerated with the same methods as steady computations.

To close the Navier-Stokes equation several RANS and hybrid RANS/LES turbulence models were implemented in FLOWer. The turbulence model equations are solved separately from the main flow equations using a full implicit time integration method. The ROT module allows body motions in translating/rotating reference frames for unsteady wind turbine simulations. FLOWer is optimized for parallel computing and uses Message-Passing Interface (MPI). A no-slip wall condition was used on the blade surface without any wall function and a far field condition was applied in the cross flow directions. For the current task the Menter SST $k-\omega$ ~~Menter (1994)~~ (Menter, 1994) based IDDES model ~~Shur et al. (2008)~~ (Shur et al., 2008) was adopted, and no transition model was considered, i.e. fully turbulent simulations were conducted. A second order dual time stepping method was adopted for the time discretisation and a five-stage Runge-Kutta scheme was used for every inner-iteration. The JST scheme was adopted for the blade meshes, and 5th order WENO scheme was adopted for the background mesh.

Block structured meshes were generated separately for the blade and background, and they were combined without sacrificing the quality of the meshes by using the Chimera overlapping grid technique ~~Chesshire and Henshaw (1990)~~(Chesshire and Henshaw, 199
. A blade mesh convergence test was performed in a previous study ~~Bangga et al. (2017)~~(Bangga et al., 2017). The blade mesh is a C-type mesh with $[280 \times 128 \times 192]$ grid cells in the chord, wall-normal and span-wise directions. The first wall-off cell

size is less than 3×10^{-6}m, which satisfies the condition $y_1^+ < 1$. The domain size was set to $[3584 \times 1792 \times 1792]\, m^3$ in the stream-wise (x) and two crossflow (y, z) directions. The rotating axis was aligned with the x axis and located at the origin, which was at a distance of 1536m from the inlet boundary. The total number of cells for simulations with the rotor were 123.5×10^6.

For the turbulent inflow cases, the wind fields were generated using the Mann turbulence generator from DTU Wind Energy. The generated turbulence field was injected at $x = -400\,\mathrm{m}$ using a momentum source term Troldborg et al. (2014) (Troldborg et al., 2014),

$$f_{Ei} = \frac{\rho u_i'}{\Delta x_n}\left(U_n + \frac{1}{2}u_n'\right)$$

where the subscript 'n' indicates the normal component to the turbulence plane. It is noted that the Gaussian convolution, which was used in Troldborg et al. (2014) (Troldborg et al., 2014) to avoid numerical oscillation, was not applied because such oscillations were not observed with the numerical scheme used near the turbulent plane, i.e. 5th order WENO. The time step was set to be approximately $1\deg$ azimuthal variation of the blades per time step. To account for controller initiated changes in rotation speed and pitch, the variations in rotation speed and pitch were recorded during BEM simulations with controller (featuring the same turbulent wind field) and prescribed to the CFD simulation via approximated Fourier series. More detail about the set-up of the CFD simulations can be found in Wenz et al. (2019); Boorsma et al. (2019b)(Wenz et al., 2019; Boorsma et al., 2019b).

For a better agreement between lifting line and CFD simulations, the airfoil data for the lifting line simulations was determined from 3D CFD simulations (Bangga et al., 2017; Bangga, 2018). To vary the angle of attack seen by the blade sections, the inflow wind speed is artificially increased/decreased by maintaining the rotational speed constant at 9.02 rpm. The effective angle of attack seen by the blade sections are then calculated using the reduced axial velocity method, often denoted as the azimuthal averaging technique, according to Hansen et al. (1997)(Hansen et al., 1997). The method takes the averaged velocity upstream and downstream of the rotor plane, and linearly interpolates the relative velocity at the rotor plane. The resulting polars include the rotational augmentation effects, hence modeling of these should be disabled in the lifting line simulations. Also the Prandtl effect due to the finite number of blades is implicitly included in the CFD simulations. Therefore the polars for the outboard sections (>70%R) are determined from 2D CFD simulations, as this effect cannot be switched off for the vortex wake simulations. Although the resulting angle of attack range covered the operational regime well for the cases under consideration, it was extended beyond that using the original polar dataset of the AVATAR turbine.

2.1.2 Bladed 4.8

The results provided by DNV GL DNV-GL are based on the BEM code of Bladed 4.8. The BEM code in Bladed 4.8 is completely rewritten and replaces the code used in Bladed 4.7 and lower. Recent public validation work is presented in references Collier and Sanz (2016) and Schepers and Boorsma (2014)(Collier and Sanz, 2016) and (Schepers and Boorsma, 2014) . The model is based on classical BEM theory where the axial and tangential Glauert momentum equations are expressed in dimensional form instead of non-dimensional factors. Further the dynamic submodels (dynamic wake, dynamic stall, skew wake correction) are fully expressed in state-space form allowing combined direct integration of structural and aerodynamic states. The aerodynamic and structural states are integrated with a 4th order variable step Runge-Kutta integrator. The engineering correction models used in the Bladed 4.8 BEM code are the Øye and Pitt&Peters dynamic wake model (described in Snel and Schepers (1994)(Snel and Schepers, 1994)), Beddoes-Leishman dynamic stall model in state-space format, Glauert skew wake correction method, Prandtl tip correction and Glauert corrections for highly loaded rotors.

Next to the classical BEM model, Bladed 4.8 and higher features a fully coupled free wake lifting line model. At present this code is used for internal purposes only and is not yet commercially released. The theory of the lifting line code is described in Kloosterman (2009)(Kloosterman, 2009). Recent work published with the code is found in Schepers and Boorsma (2014) and Harrison et al. (2018)(Schepers and Boorsma, 2014) and (Harrison et al., 2018). The implementation in Bladed is however fully coupled to the Bladed multibody model and allows for aeroelastic load simulations. For the turbulent inflow test cases, a time step which is approximately equivalent to 1 step per degree of revolution was applied. Special effort has been made to ensure efficient parallelization and vectorization of the code. It is also possible to distinguish between wake update frequency and aerodynamic time step, which has a great potential for reduction of computational time Boorsma et al. (2019a) (Boorsma et al., 2019a).

2.1.3 Phatas

The computer program Phatas, 'Program for Horizontal Axis wind Turbine Analysis and Simulation' Lindenburg and Schepers (2000), is developed for the time-domain calculation of the dynamic response and the corresponding loads on a Horizontal Axis wind Turbine. The program Phatas is available as tool in the integrated wind turbine design package FOCUS6 foc (2016). The program Phatas has its own 'internal' BEM based aerodynamic model but is also available in a configuration **PhatAero** that uses the aerodynamics from an external module such as ECN Aero Module.

The internal BEM based aerodynamic model features several engineering extensions such as a dynamic inflow model Snel and Schepers (1994), yaw model Schepers and Vermeer (1998); Schepers (1999), root and tip loss model Prandtl and Betz (1927) and a turbulent wake state model based on the formulation of Wilson. For the airfoil data, the modeling of dynamic stall behaviour Snel (1997) and rotational effects on lift Snel et al. (1993) are optional based on Snel's models. The internal model features a recent addition to account for the effects of shed vorticity (Blade Shed Vorticity), which calculates a vortex structure of shed vorticities based on the time history of the lift coefficients and the relative velocities of the airfoils Boorsma et al. (2019a).

The aerodynamic properties of the blade were modelled with the Cl-Cd-Cm tables derived from the CFD calculations of the University of Stuttgart. The options for correction of the lift coefficient for the effects or rotation ('3D effects') was not used. There was no model for dynamic stall used. The blades were modelled with 31 elements over the span, where 29 elements have equal length and the 2 elements close to the tip have half that length. The aerodynamic stagnation from the tower was not included. The time increment was set to give a 1° increment in rotor azimuth.

The input settings of phatAERO + ECN Aero Module AWSM are for a 6 diameter total wake length of which 2 diameters are for a free-geometry wake length. The calculations were done with the option to skip the 'odd' aero calls, which reduces the number of aerodynamic evaluations and likewise reduce the CPU needed. The simulations featuring the Blade Shed Vorticity model (indicated by Phatas-BSV) incorporate the effect of 20 shed vortices.

2.1.3 ECN Aero Module

The ECN Aero Module Boorsma et al. (2011, 2016b) (Boorsma et al., 2011, 2016b) includes two aerodynamic models, the BEM method similar to the implementation in PhatasLindenburg and Schepers (2000) (Lindenburg and Schepers, 2000) and a free vortex wake code in the form of AWSMvan Garrel (2003)(van Garrel, 2003). Both models are lifting line codes, i.e. they make use of aerodynamic look-up tables to evaluate airfoil performance. The set-up allows to easily switch between the two aerodynamic models whilst keeping the external input the same, which is a prerequisite for a good comparison between them. Although the package can be coupled to simulation software that solves the structural dynamics of a wind turbine (FOCUS foc (2016), SIMPACK sim (2018)(foc, 2016), SIMPACK (sim, 2018)), the stand-alone option is used simulating a rigid turbine with prescribed operational conditions. The BEM model features a local implementation, i.e. solving the momentum equations separately for each blade element rather than once for a full annulus. Several engineering extensions are used such as a dynamic inflow model Snel and Schepers (1994)(Snel and Schepers, 1994), yaw model Schepers and Vermeer (1998); Schepers (1999) (Schepers and Vermeer, 1998; Schepers, 1999), root and tip loss model Prandtl and Betz (1927) (Prandtl and Betz, 1927) and a turbulent wake state model (replacement of the theoretical momentum equation with a linear relation between thrust coefficient and axial induction factor above a value of 0.38 for this parameter).

The Snel first order dynamic stall model Snel (1997) (Snel, 1997) was applied to all simulations (unless stated explicitly otherwise) and rotational corrections were disabled. For the free vortex wake simulation, the number of wake points was chosen to make sure that the wake length was developed over at least 3 rotor diameters downstream of the rotor plane. The wake convection was free for the first 2 wake diameters downstream of the rotorplane. For the remaining wake length, the blade averaged induction averaged induction (for each blade vortex sheet) at the free to fixed wake transition is applied to all wake points. For both aerodynamic solvers approximately 20 elements in spanwise direction were used. The spanwise discretization in AWSMfeatures approximates a cosine distribution, whereas this is linear for BEM featuring half the spacing at the tip. For the turbulent inflow calculations, the time step was kept at the approximate equivalent of 1° azimuth for both the BEM and AWSM simulations. Wake reduction Boorsma et al. (2018) (Boorsma et al., 2018) (reducing the shed vorticity spacing) was applied after approximately half a diameter convected wake, skipping 9 shed vortices to end up with an effective distance of 10° azimuth between the shed vortices in the remaining part of the wake. This typically results in about 500 streamwise wake points and hence about $500 \cdot 20 \cdot 3 = 30000$ vortex filaments for a simulation.

2.1.4 Phatas

The computer program Phatas, 'Program for Horizontal Axis wind Turbine Analysis and Simulation' (Lindenburg and Schepers, 2000) , is developed for the time-domain calculation of the dynamic response and the corresponding loads on a Horizontal Axis wind Turbine. The program Phatas is available as tool in the integrated wind turbine design package FOCUS6 (foc, 2016). The program Phatas has its own 'internal' BEM based aerodynamic model but is also available in a configuration **PhatAero** that uses the aerodynamics from the coupled ECN Aero Module.

The internal BEM based aerodynamic model features several engineering extensions such as a dynamic inflow model (Snel and Schepers, 1994), yaw model (Schepers and Vermeer, 1998; Schepers, 1999), root and tip loss model (Prandtl and Betz, 1927) and a turbulent wake state model based on the formulation of Wilson. For the airfoil data, the modeling of dynamic stall behaviour (Snel, 1997) and rotational effects on lift (Snel et al., 1993) are optional based on Snel's models. The internal model features a recent addition to account for the effects of shed vorticity (Blade Shed Vorticity), which calculates a vortex structure of shed vorticities based on the time history of the lift coefficients and the relative velocities of the airfoils (Boorsma et al., 2019a).

The blades were modelled with 31 elements over the span, where 29 elements have equal length and the 2 elements close to the tip have half that length. The aerodynamic stagnation from the tower was not included. The time increment was set to give a 1 ° increment in rotor azimuth.

The input settings of PhatAero + ECN Aero Module AWSM are for a 6 diameter total wake length of which 2 diameters are for a free-geometry wake length. The calculations were done with the option to skip the 'odd' aero calls, which reduces the number of aerodynamic evaluations and likewise reduce the CPU needed. The simulations featuring the Blade Shed Vorticity model (indicated by Phatas-BSV) incorporate the effect of 20 shed vortices. A high level overview of the codes used is given in Table 1.

Table 1. High level overview of codes and settings

Code	USTUTT	DNV-GL		LM Windpower			TNO	
	FLOWer	Bladed4.8		PhatasSV‡	PhatAero		ECNAero	
	CFD	BEM	VL	BEM	BEM	AWSM	BEM	AWSM
Dynamic stall	-	Bed-Leis	Bed-Leis†	-	-	-	Snel 1st order§	Snel 1st order
Dynamic inflow*	-	Øye	-	ECN	ECN	-	ECN	-
Yawed flow	-	Glauert	-	Schepers	Schepers	-	Schepers	-
Time step [° azi]	1	1	1	1	1	1	1	1
Wake length [Diam]	17	-	5	-	-	6	-	3

‡ PhatasSV-BSV is also used which contains a separate shed vorticity model † Shed vorticity effects excluded for vortex wake simulations
§ Beddoes Leishman model was used for several cases (ECNAero-BEM-BL) * See text for implementation differences

2.2 Constant uniform and sheared inflow

Four uniform inflow cases were simulated following part of the power curve, as summarized in Table 2. The resulting load comparison is given in Figure 1 for the radial distribution of ~~chordnormal~~ chord normal and tangential force, plus the deduced integral aerodynamic variables axial force, and power. It is observed that generally speaking a good agreement is found between lifting line and CFD simulations, which is attributed to the polars being generated from 3D CFD simulations as described in

Table 2. Summary of uniform and sheared inflow comparison cases

Case type	Wind speed U_∞ [m/s]	Pitch angle [°]	Rot. speed [rpm]	Shear expon. [-]	Tip speed ratio λ [-]	Angle of attack $\alpha^\dagger$@80%R [°]	Axial ind. factor $a^\dagger$@80%R [-]
uniform	4.0	0.00	6.0000	-	16.2	-1.0	0.28
uniform	5.0	0.00	6.0000	-	12.9	-0.1	0.25
uniform	6.0	0.00	6.0000	-	10.8	0.9	0.23
uniform	8.0	0.00	6.8738	-	9.3	1.9	0.21
shear	10.5	0.00	9.0218	0.2	9.26	1.7	0.20
shear	14.0	6.06	9.6000	0.2	7.39	-1.4	0.04

† estimate

section 2.1.1. The good agreement is a prerequisite for a successful comparison of unsteady aerodynamics in sheared and turbulent inflow conditions.

In addition to that, also two vertically sheared inflow cases were simulated (see also Table 2). Looking at the flapwise blade root moment variation in Figure 2b we can observe differences between the predicted amplitudes of the codes. These differences grow larger for the underlying axial induced velocities in Figure 2a. Here it is noted that 'lifting line variables' such as angle of attack and induced velocities are not available for the CFD results and hence are not displayed.

~~Load comparison in uniform inflow conditions~~

~~Azimuthal variation and amplitudes in shear, U_∞=10.5 m/s~~

To better observe the differences the simulation results are post-processed to average values and amplitudes (by evaluating the difference between maximum and minimum values) of the fluctuation along a rotor revolution. The remaining plots of Figure 2 show the results of the amplitude comparison and here we do observe a striking difference between vortex wake and BEM type codes. The BEM type codes systematically over predict the amplitudes of the normal forces in comparison to the CFD and vortex wake results (that are in relatively good agreement), consistent along the blade span except for the most inboard station at 30%R. The difference can be traced back to the angle of attack and the underlying axial induced velocity variation in Figure 2d, which can be considered as the 'heart' of lifting line models. For the vortex wake codes, the axial induced velocity follows more extremely the inflow velocity variations as the blades rotate through the sheared velocity field. Between the BEM codes it can also be observed that whereas some of them predict a substantial azimuthal variation of axial induced velocity, there are also BEM results where this azimuthal variation along a rotor revolution is almost negligible. It is known that a wide variety of BEM implementations exist, e.g. solving the momentum equations for a whole annulus or per element, not to mention the interaction with a dynamic wake or dynamic inflow model. This example illustrates the effect these implementation differences can have. Application of the dynamic inflow model to the local element induced velocity (as implemented in the Bladed4.8-BEM results following the TUDK model as described in ~~Snel and Schepers (1994)~~ (Snel and Schepers, 1994)) appears to dampen out induced velocity variations in non-uniform inflow conditions. The other

BEM codes use a similar dynamic inflow model, but the dynamic inflow term is related to the annulus averaged induced velocity rather than its respective element value, which results in better tracking of inflow variations.

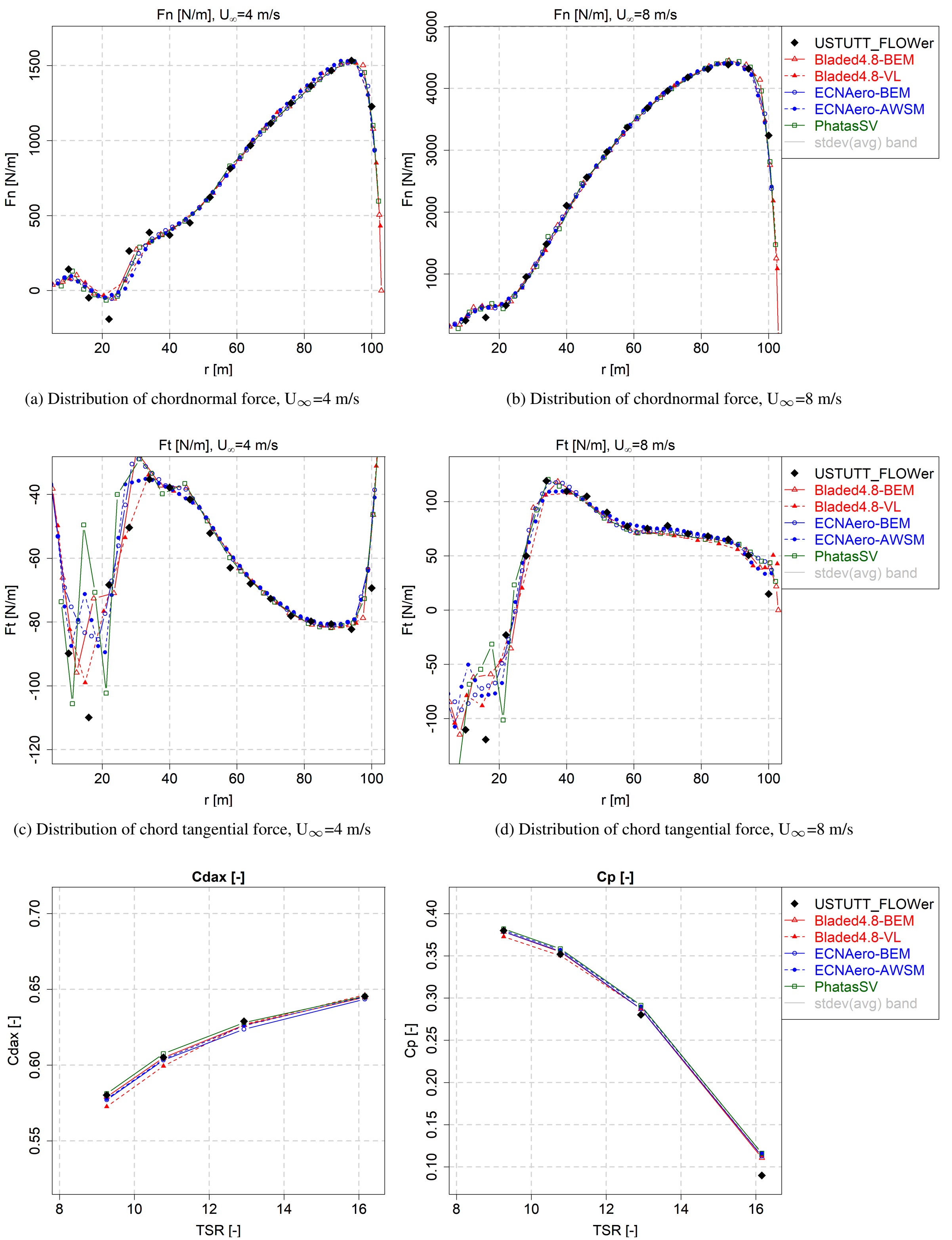

(a) Distribution of chordnormal force, U_∞=4 m/s

(b) Distribution of chordnormal force, U_∞=8 m/s

(c) Distribution of chord tangential force, U_∞=4 m/s

(d) Distribution of chord tangential force, U_∞=8 m/s

(e) Axial force coefficient Cd_{ax}

(f) Power coefficient Cp

Figure 1. Load comparison in uniform inflow conditions

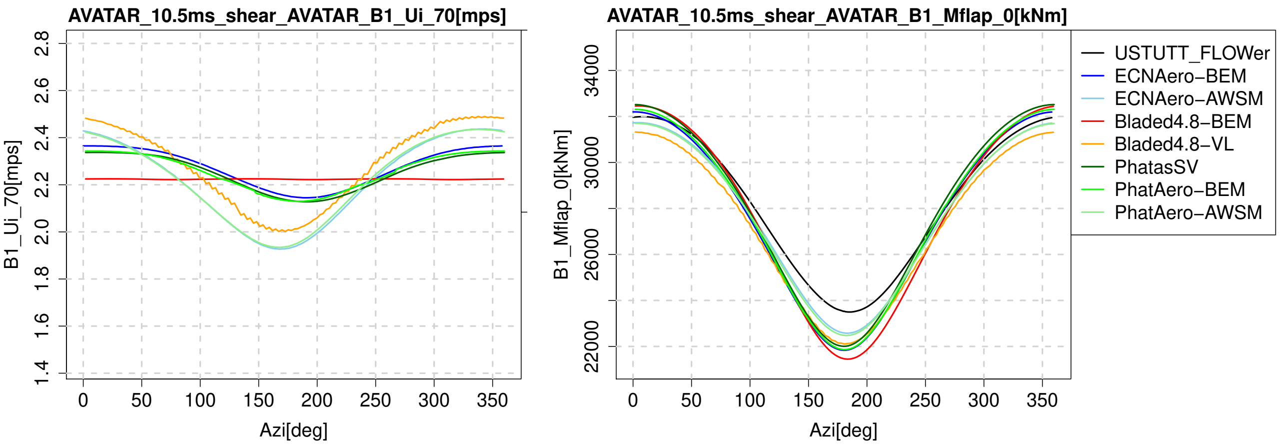

(a) Azimuthal variation of axial induced velocity Ui, 70%R

(b) Azimuthal variation of flapwise blade root moment Mflap

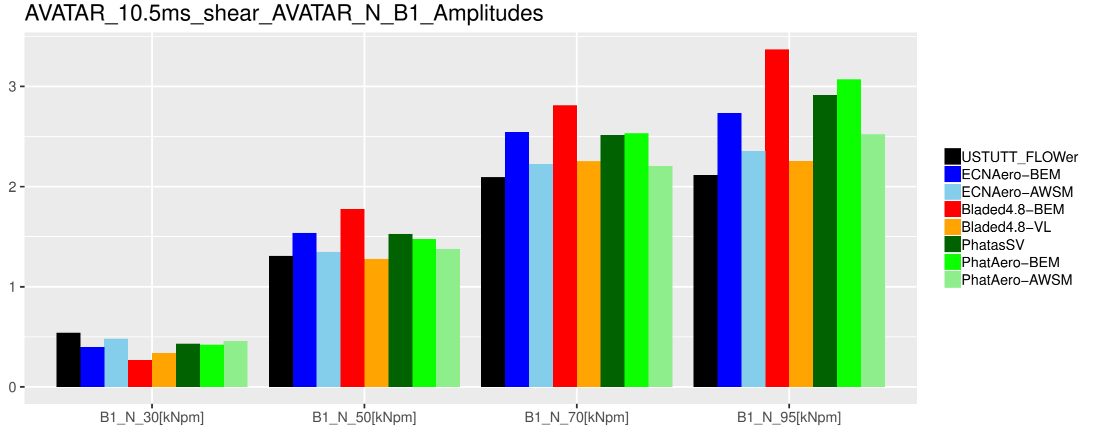

(c) Amplitudes of chordnormal force along the blade span at 30%R, 50%R, 70%R and 95%R

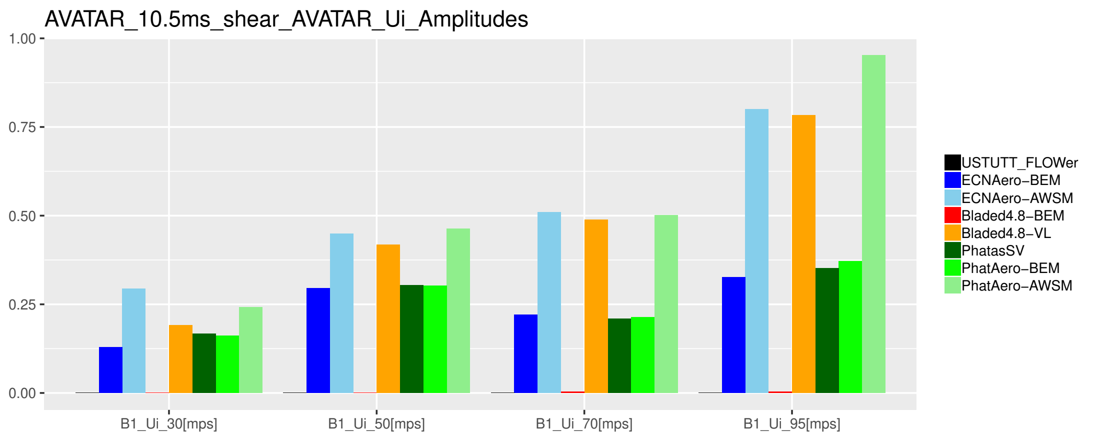

(d) Amplitudes of axial induced velocities along the blade span at 30%R, 50%R, 70%R and 95%R

Figure 2. Azimuthal variation and amplitudes in shear, U_∞=10.5 m/s

In search of a fundamental reason for the difference between BEM and vortex wake codes, calculations were done for various conditions ~~with the Phatas~~ (ranging between 6 m/s and 18 m/s wind speed) with the PhatasSV and PhatAero code. These ~~conditions also include~~ calculations also included 2-bladed and 4-bladed versions of the AVATAR rotor. For the 2-bladed rotor models the chord distribution is simply 1.5 times larger compared to the chord distribution of the 3-bladed rotor. The 4-bladed rotor model has 75% of the chord distribution compared to the 3-bladed rotor. This 'scaling' gives a similar rotor disk loading except near the blade tip. For all configurations the solidity of the rotor is 0.0408. The result shows that for all operational conditions the 1P variation of the blade root flap moment from the BEM based calculations is larger than from the AWSM calculations. This seems to be related to the axial induction factor, see also Figure 3. Although the values of the axial induction factor are not distributed homogeneously, a nearly ~~linear trend follows of~~ quadratic trend follows for the ratio between blade root flapwise bending moment variation from BEM simulations compared to the vortex wake (AWSM) simulations. The ratio between root moment variations shows to be quite insensitive to the number of rotor blades or the distance between the vortex sheets of the blades.

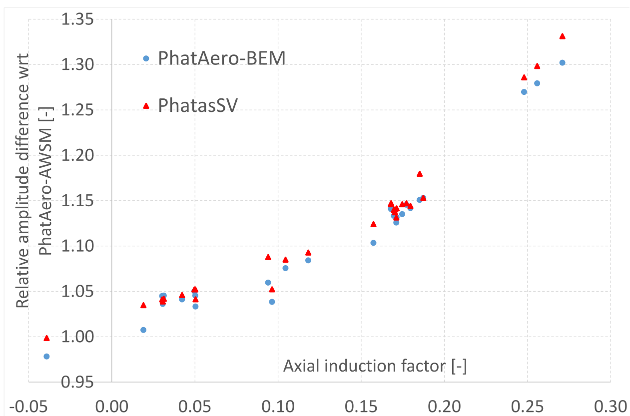

Figure 3. Relative difference of Mflap amplitudes from BEM calculations in shear w.r.t. PhatAero-AWSM versus axial induction factor

2.3 Turbulent inflow

After exposing the differences between the codes in sheared inflow, the next step is a comparison in turbulent inflow. Six cases were simulated, as summarized in Table 3. To ensure all partners reads the turbulent wind file in the same way and signal processing is in agreement amongst the partners, first an alignment study was performed using a 150 s simulation from the EU AVATAR project ~~Kim et al. (2016)~~(Kim et al., 2016), which featured a constant pitch and rotational speed at an average hub height wind speed of 10.5 m/s. The cases summarized in Table 3 are defined in agreement with IEC Class 1A, ~~where~~ although wind shear was excluded from the comparison. The first case featured a constant rotational speed and pitch angle at 8 m/s hub height wind speed. For the AVATAR turbine the class 1A specification leads to a rather high turbulence intensity of 23% and a length scale of 33.6 m. Seed selection was determined by running six different seeds with BEM and matching the most representative seed to the average values of fatigue, mean and standard deviation over the six seeds. Wind field duration

Table 3. Turbulent inflow comparison cases

Nr [-]	Case	Hub wind [m/s]	Turb. intensity [%]	Length scale [m]	Rot. speed [rpm]	Pitch angle [deg]	Wind seed [-]	Duration [s]
1	8ms_fixed	8	~23	33.6	6.87	0.0	205	400
2	8ms_prscrbd	8	~23	33.6	prscrbd	0.0	205	400
3	16ms_prscrbd	16	~17	33.6	prscrbd	prscrbd	205+offset	200
4	8msTI10_prscrbd	8	~10	33.6	prscrbd	0.0	205+scale	400
5	8msCt_prscrbd	8	~23	33.6	prscrbd+1.5	-1.5	205	400
6	8msL_prscrbd	8	~23	134.4	prscrbd	0.0	208	400

was set to 400 seconds (16 m/s case excepted) based on a compromise between computational expense and a good statistical representation. For the second case, a BEM simulation with the AVATAR controller activated was performed with the wind seed under investigation. The resulting rotational speed and pitch angle variations were recorded and fed to the CFDsimulation CFD, BEM and vortex wake simulations (this is indicated by the suffix 'prscrbd'). The same procedure was adopted for the other cases. Since the wind speed was below rated, the resulting pitch angle remained constant for this case at 0°. For the third case the same wind seed was used but the offset was increased to result in an average of 16 m/s hub height wind speed. Acknowledging that a wind seed turbulence box has a constant length, doubling the wind speed effectively means that the simulation duration is halved to 200s. In agreement with IEC Class 1A specifications, the wind speed fluctuations were scaled to match an average turbulence intensity of roughly 17%. For the fourth case, the influence of varying the turbulence intensity was investigated by scaling the amplitude of fluctuations for the same seed to approximately 10%. For the fifth case, the influence of an increased thrust coefficient or axial induction factor was investigated. To this means an offset was applied to the rotational speed and pitch angle variation of the second case. This way the operating angle of attack was not significantly different from the second case and the spanwise variation of the averaged axial induction remained relatively constant. Finally for case six, the influence of a different length scale was investigated by increasing this parameter with a factor of four. The idea behind this case is to mimic the effect of rotor size by changing the turbulence length scale. It is anticipated that the rotational sampling will be different between small and larger rotors, influencing the coherence of the encountered wind gusts. For more info on the case description, please consult the dedicated report from University of Stuttgart Wenz et al. (2019) (Wenz et al., 2019) on this subject.

2.3.1 Comparison methodology

In cases with turbulent inflow, besides a statistical evaluation, analysing the development of forces over time is an interesting approach which might give more insight. In order to do this a consistent input of background turbulence in the different codes has to be ensured. In CFD, turbulence is altered as it propagates through the domain until it reaches the rotor, while in BEM and vortex wake models, the flow field, i.e. turbulence, is applied directly to the rotor. Moreover, the propagation in CFD is slowed down in front of the turbine due to the rotor blockage. To allow a time-dependent load comparison between the codes these CFD effects need to be compensated in the lifting line code input. This was achieved by extracting the turbulent velocity field from the empty box CFD simulations and applying a time shift to compensate for the blockage effect. A detailed explanation of the method is given elsewhere ~~Wenz et al. (2020, 2019)~~ (Wenz et al., 2020, 2019)

The resulting alignment between the codes was verified by comparing the values of the encountered wind by the blades using virtual 'wind probes' at several radial stations. Generally speaking a good agreement of the encountered wind variation as a function of time was found using this method, indicating that the turbulence structures from empty box and rotor CFD are highly alike, providing similar fluctuations due to the rotational sampling. However it should be realized that although this method comes close, definition of identical inflow conditions between CFD and lifting line codes is impossible and the current approach is an approximation based on an engineering method. As such small inflow differences between lifting line codes and CFD remain.

2.3.2 Differences between the models

To study the differences between the codes the statistics (minimum / maximum / average / standard deviation) over the full time ~~serie~~ series were determined as well as the 1Hz equivalent loading (based on the rainflow counting procedure using a slope of m=11) for a large number of variables. Despite the small differences in inflow definition, the 8 m/s fixed case (i.e. fixed rotational speed and pitch angle) allows to draw some interesting conclusions with respect to the effects of modeling differences. A summary of key results from ~~the 8 m/s (fixed rotational speed and pitch angle)~~ this case are shown in Figure 4. In agreement with results from the AVATAR project and the sheared inflow comparison, the induced velocity variation of vortex wake models follows more directly the underlying inflow variations than the BEM results. The vortex wake model from Bladed features the same behavior as the previously studied vortex wake models. As a result, the fluctuations in angle of attack and consequently aerodynamic loads are smaller (within the sectional velocity triangle the change in wind speed is partly compensated by the change in axial induction). This is clearly affecting the equivalent sectional load levels at all radial stations (inboard at 30%R often excepted) and hence also the blade root moments. The comparison to CFD indicates that generally speaking the vortex wake codes agree better with CFD than BEM judging by the magnitude of load fluctuations and resulting equivalent load levels.

From previous work ~~Boorsma et al. (2016a)~~ (Boorsma et al., 2016a) it was hypothesized that part of the observed difference between BEM and vortex ~~type~~ wake codes can be explained by the shed vorticity modeling which is implicitly included for vortex wake models but not in BEM. A dedicated model to simulate the effect of shed vorticity changes has been developed for the Phatas PhatasSV code, called Phatas-BSV, see also section 2.1.4. It is also noted that the indical method from Beddoes & Leishman Leishman and Beddoes (1986, 1989) (Leishman and Beddoes, 1986, 1989) for modeling unsteady sectional aerodynamics includes a part dedicated to modeling shed vorticity effects based on Theodorsen's theory Theodorsen (1935)(Theodorsen, 1935). As alternative to Snel's dynamic stall model, this submodel was applied in the ECN Aero Module (ECNAero-BEM-BL). The resulting fatigue equivalent blade root moments displayed in Figure 5 indeed confirm that modeling shed vorticity partly reduces the discrepancy between BEM and vortex wake codes. In addition to that it is observed that both the blade shed vorticity model in Phatas PhatasSV (which acts on the induced velocities by modelling a shed vorticity structure) and the Theodorsen part of the Beddoes Leishman (which acts on the airfoil coefficients rather than induced velocities) result in a similar effect on the fatigue equivalent moments.

Studying the axial induced velocity variations in Figure 4a reveals not only large differences between BEM and vortex wake type codes, but also between the different BEM codes. Where the red line shows a nearly constant level, the other BEM codes feature more variation with inflow velocity. This was also observed in the sheared inflow comparison as described in section 2.2, where an explanation for the differences between the BEM codes was given. . Here this difference was found to be related to the various implementations of the dynamic wake or dynamic inflow model, which can result in dampening of induced velocity variations due to inflow fluctuations.

Key results for the U_∞=8 m/s fixed rotational speed and pitch angle case

Effect of shed vorticity modeling on fatigue equivalent flapwise blade root moment (U_∞=8 m/s fixed)

2.3.3 Effect of load case variations

For several cases the earlier mentioned small differences in inflow conditions between CFD and lifting line codes influence the equivalent load levels, as the result of the rainflow counting is dominated by the largest fluctuation over the time series. Therefore it is decided to study the staircase plots from the rainflow counting procedure, which are an intermediate result showing the range of fluctuations versus the number of occurrences or counts. Instead of focusing on the equivalent load level determined by the largest ranges with very few occurrences, statistically it makes more sense to study the ranges with a large number of counts when comparing CFD to lifting line simulations. To compare the results between the codes over the simulated load cases, the staircase plots of the flapwise blade root moments (e.g. Figure 4c) were integrated (starting at a threshold of 10 counts, keeping the logarithmic distribution for the number of counts). A summary of the results is given in Table ??. Relative difference of staircase plot integrated (INT) and fatigue equivalent (EQL) flapwise blade root moments† Case ECNAero-BEM ECNAero-BEM-BL ECNAero-AWSM ECNAero-BEM ECNAero-BEM-BL%%%%%8ms_fixed 22.2 10.0 1.4 13.8 8.9 8ms_prserbd 29.6 11.2 5.6 12.5 5.416ms_prserbd 31.6 9.2 12.68.5 -1.68msTI10_prserbd 26.1 8.5 2.814.0 8.08msCt_prserbd 34.8 13.4 0.819.4 11.08msL_prserbd 30.1 11.4 6.414.9 7.5† Averaged over 3 blades, staircase plots integrated from a threshold value of 10 counts. Figure 6

In agreement with the results of the 8m/s fixed case, the vortex wake results tend to agree well with CFD also for the other cases. Drawing general conclusion on variations between the load cases is complicated because observed differences between the cases can potentially be caused by the difference in specific turbulence boxes (seeds) and the way the rotor blades slice through them. It seems that similar to the shear case, a higher thrust coefficient value results in larger differences between BEM on the one hand and vortex wake / CFD models on the other hand. The 16 m/s result features a very low thrust (axial induction factor around 0.06), which makes the BEM with shed vorticity modeling come very close to the vortex wake model, although a rather high unexplained difference remains with CFD. Simulating a higher length scale (mimicking a 4 times smaller turbine) unexpectedly seems to have hardly any impact on the magnitude of the differences between the models.

Although comparison of equivalent loads between CFD and lifting line codes is hindered by small differences in inflow conditions, a comparison between lifting line codes (BEM and vortex wake) in terms of fatigue loading is deemed useful in the last two columns of Table ??. Figure 6b. These numbers also confirm that the shed vorticity modeling in BEM for this 16 m/s case make these results come very close to the vortex wake results. And this difference to be at maximum for the high thrust case. It can also be observed that, although the absolute level of the flapwise fatigue load will decrease with a lower turbulence intensity, the relative difference between BEM and vortex code type wake code results remains similar. For more details the full report Boorsma et al. (2019b) (Boorsma et al., 2019b) about the comparison between lifting line and CFD simulations can be consulted.

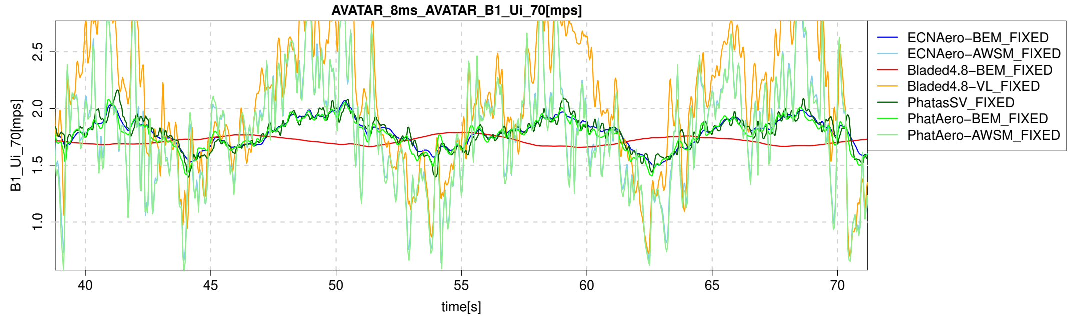

(a) Time trace of axial induced velocity at 70%R

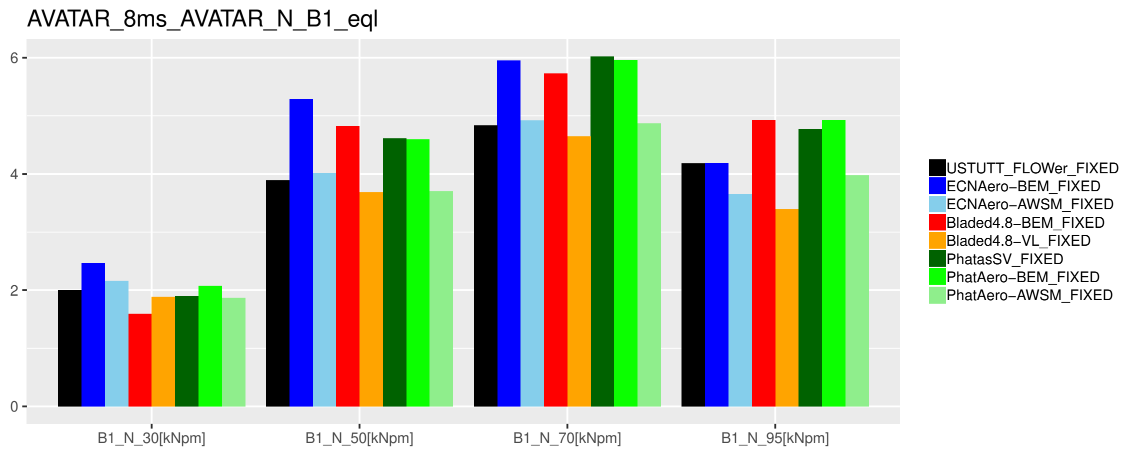

(b) Fatigue equivalent of chordnormal force at 30%R, 50%R, 70%R and 95%R

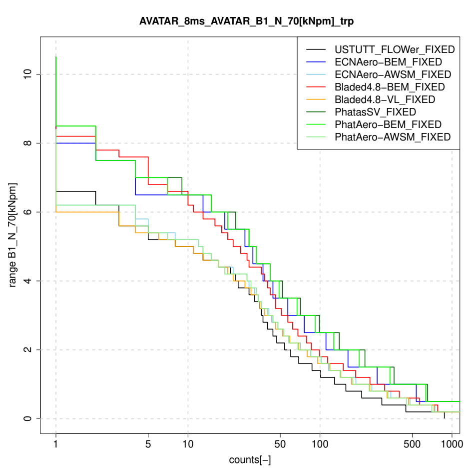

(c) Staircase plot of chordnormal force at 70%R

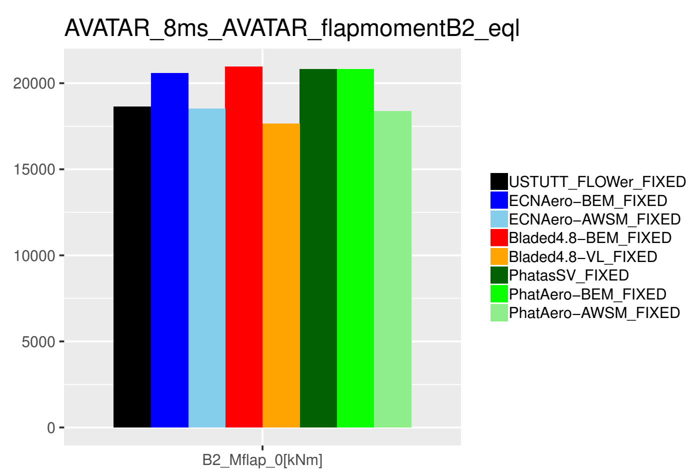

(d) Fatigue equivalent flapwise blade root moment

Figure 4. Key results for the U_∞=8 m/s fixed rotational speed and pitch angle case (first case from Table 3)

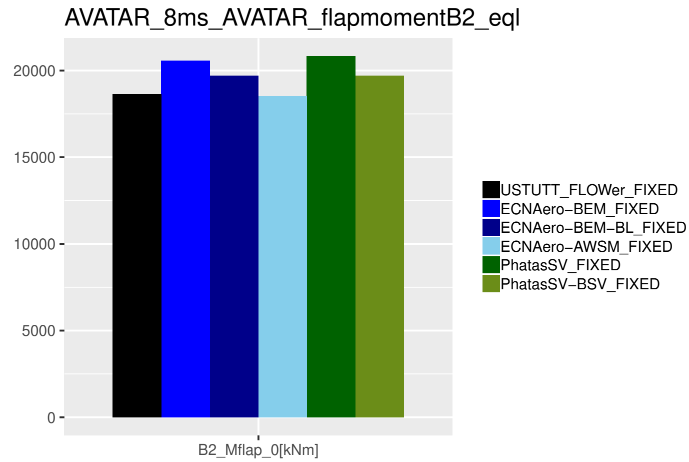

Figure 5. Effect of shed vorticity modeling on fatigue equivalent flapwise blade root moment for the first case from Table 3 (fixed rotational speed). The legend addition 'BSV' stands for the blade shed vorticity model in PhatasSV, while 'BL' indicates usage of the Beddoes Leishman instead of the Snel model for unsteady airfoil aerodynamics.

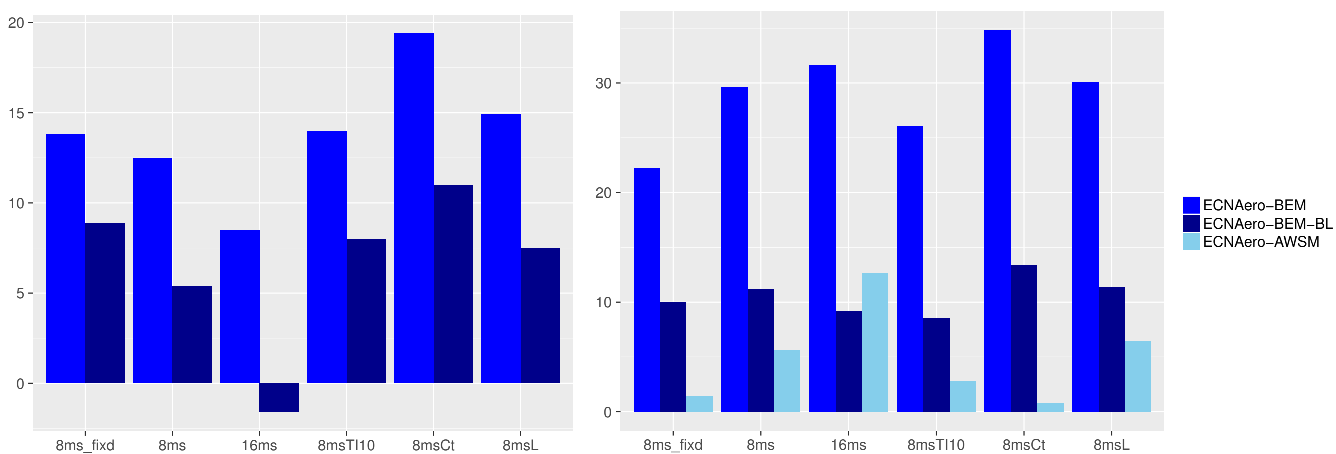

(a) EQL relative to ECNAero-AWSM %

(b) INT relative to USTUTT_FLOWer in %

Figure 6. Relative difference of fatigue equivalents (EQL) and integrated staircase plot values (INT) of flapwise blade root moments for the turbulent inflow cases. Values are averaged over 3 blades, staircase plots integrated from a threshold value of 10 counts.

2.4 Improved induction tracking

From section 2.2 it appeared that a ~~structural~~ difference exists between the predicted load fluctuation amplitudes in vertical shear from vortex wake (AWSM) and BEM type codes, which correlates with the axial induction factor. Application of an engineering extension to BEM, accounting for the effect of shed vorticity variation did not yield an explanation for this difference. Most likely the gradual inflow variations in vertical shear are not abrupt enough for the shed vorticity variation to play an important role. In turbulent inflow (see also Figure 5), shed vorticity and dynamic inflow can explain part of the observed differences between BEM and vortex wake modeling. In an attempt to further study the cause for the remaining difference, results from BEM and vortex wake sheared inflow simulations on the AVATAR rotor have been post-processed to verify compliance with the axial momentum equations. The one dimensional axial momentum equations constitute a relation between the thrust coefficient Ct and the axial induction factor a at the rotor disc in the form of

$$\mathrm{Ct} = 4\mathrm{a}(1-\mathrm{a}) \quad \text{and} \quad \mathrm{a} = \mathrm{Ui}/\mathrm{U} \quad , \tag{1}$$

with

Ct	[-]	thrust coefficient
a	[-]	axial induction factor at the rotor disk
Ui	[m/s]	axial induced velocity
U	[m/s]	wind speed.

It is noted that Ct is based on the force of a single blade element and a the axial induction for the corresponding annulus, hence corrected for the finite number of blades using the Prandtl tip loss factor (BEM) or by averaging the induced velocities over the annulus (AWSM). To be able to focus on the effect of shear a relatively large shear exponent of 0.75 at 8 m/s hub height wind speed was employed for the investigation. The results in Figure 7a indicate that the BEM simulation complies with the underlying momentum equation as it is supposed to. However the vortex wake results in Figure 7b clearly deviate from this line depending on the azimuthal position, where especially for the outboard stations high thrust coefficients are obtained in combination with a relatively low axial induction factor (lower as would be the case for the theoretical momentum line) for a downward pointing blade featuring the lowest local inflow velocity. It can be shown that for rotors operating at higher induction, BEM theory can even predict an increase rather than decrease in axial induced velocity when the blade is pointing downward (6 o' clock position), due to the fact that for the relative high local thrust coefficient the corresponding axial induction factor increase is larger than the local wind inflow decrease (a=Ui/U). This is unlikely to be the case in reality (non-physical), which is backed up by the fact that corresponding vortex wake calculations predict the opposite trend, namely the axial induced velocities to decrease for a lower local inflow speed at the downward pointing blade position.

Acknowledging the fact that the vortex wake model does not obey the momentum equations as implemented in BEM theory, one may reflect on which shortcoming of BEM theory is responsible for this difference. Several assumptions are made in the derivation of BEM theory and an inventory was made which specific violations of this theory occur in sheared inflow.

- Radial independence

  The influence of neighbouring elements and of the other blades are not taken into account and each annulus is treated separately. For a spanwise uniform circulation distribution it is acknowledged that intermediate trailed vorticity effects are absent and as long as the loading differences between the blades are not significant this effect can be neglected as well.

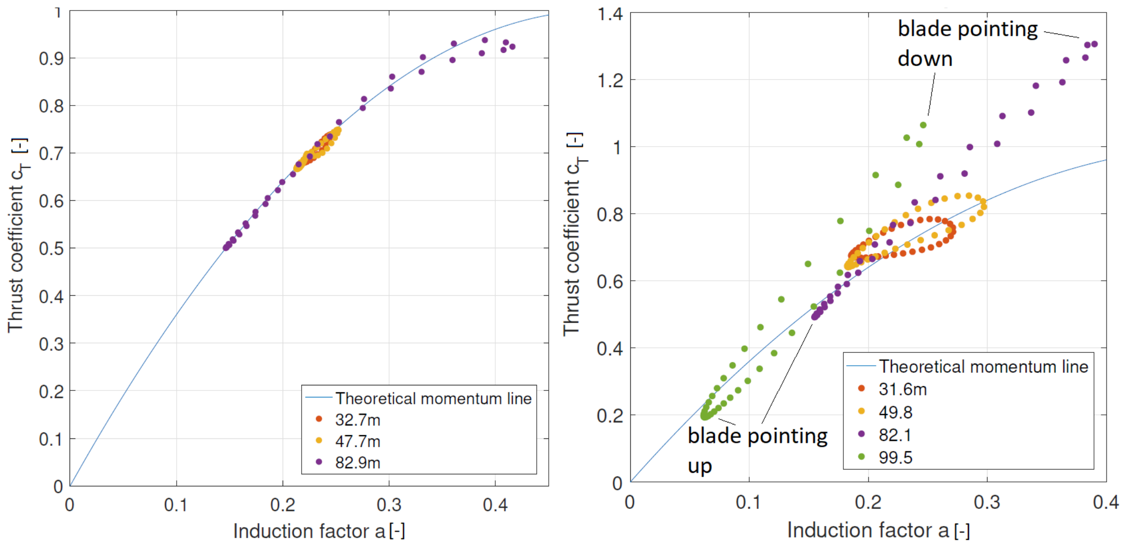

(a) BEM (element approach)

(b) AWSM vortex wake

Figure 7. Comparison of post-processed AVATAR rotor simulation results in heavy shear (U=8 m/s, $\alpha = 0.75$) for several radial stations against the theoretical momentum line

However in sheared inflow, even for a blade that is designed with uniform spanwise circulation distribution, a varying spanwise circulation distribution will result in trailed vorticity which violates the radial independence assumption.

– Axi-symmetric or uniform inflow conditions

It is well known that BEM theory assumes steady inflow conditions, which relates to the variation of wind velocity along the longitudinal direction of the streamtube. In addition to this the derivation of the underlying one dimensional axial momentum equation assumes that the inflow conditions are axi-symmetric (or uniform) with respect to the streamtube considered. In sheared inflow conditions (or any other non-uniform inflow condition such as turbulent or waked inflow) it may be clear that this is not the case. It was shown previously that the Betz limit can be exceeded in non-uniform inflow conditions ~~Chamorro and Arndt (2013)~~(Chamorro and Arndt, 2013). The implication of the violation of axi-symmetric or uniform inflow conditions may differ between a BEM approach that solves the momentum equations 'annulus averaged' (i.e. using one equation resulting in the same induced velocity for all the blades) or the more modern local approach that solves the momentum equation separately for each blade. In the latter case one may ask the question what the azimuthal and radial extent of the streamtube is, that balances the force exerted by a blade.

Further consideration of the second violation aspect triggered the idea to distinguish between the wind velocity used in BEM for the purpose of evaluation of the sectional force (~~blade element part) and~~ U_e, blade element equations) and for the determination of induced velocity (U_m, momentum equations). See also the below displayed axial momentum equation 2 ~~, assuming that the tangential induction can be ignored.~~ (for the sake of simplicity the tangential induction and a correction for the finite number of blades have been removed here).

$$2\mathrm{a}(1-\mathrm{a})\rho \mathrm{U}_m{}^2 2\pi r dr = \sum_B c0.5\rho W^2 c_l(\alpha)\cos(\phi)dr \quad , \tag{2}$$

where

$$\phi = atan2(\sout{W}\mathrm{U}_e(1-\mathrm{a}),\Omega r), \quad \alpha = \phi - \epsilon \quad \text{and} \quad W = \sout{\sqrt{\mathrm{U}^2(1-\mathrm{a})^2+(\Omega r)^2}}\sqrt{\mathrm{U}_e{}^2(1-\mathrm{a})^2+(\Omega r)^2}$$

with

U_e	[m]	wind speed used for blade element equation
U_m	[m/s]	wind speed used for momentum equation
r	[m]	radius of element considered
c	[m]	local blade chord at radius r
ρ	[kg/m^3]	air density
W	[m/s]	effective velocity at element
c_l	[-]	lift coefficient
α	[$^\circ$]	angle of attack
ϕ	[$^\circ$]	inflow angle wrt rotor plane
Ω	[rad/s]	rotor speed
ϵ	[$^\circ$]	twist plus pitch angle ~~and torsion deformation~~ (and possible torsion deformation)

In this equation the blade element part is on the right hand side, in which the wind velocity U_e is included through the effective velocity term W, the inflow angle ϕ and angle of attack α. The momentum part is on the left hand side of equation 2. It is noted that in the so called 'annular average' BEM, the element forces are summed over the blades ($\sum_B$) and the corresponding annulus has a 360° extent, resulting in a single axial induction factor for all blades. The current 'element 'BEM implementation which is used here solves equation 2 for each blade separately (adjusting the annular volume correspondingly), resulting in different induced velocities for each blade element in an annulus.

Revisiting the idea to distinguish between the wind velocity used in BEM for the purpose of evaluation of the sectional force (blade element part) and the determination of induced velocity (momentum equations), it is clear that the local wind velocity acting at an element quarter or three-quarter chord point should be used for the first part. For the second part it could be argued to use a wind speed that is representative for the streamtube considered instead of a local point at the element center (as it is currently implemented). The question is how to define this streamtube and how to define a representative wind speed for it. Where a CFD or vortex wake simulation considers all spatial wind speed variations by means of a mesh, the momentum theory in BEM allows for only one. Effectively this is an inherent shortcoming of BEM and it could be argued we have arrived at a limitation that cannot be overcome. In a first attempt a streamtube is defined that considers an annular sector with azimuthal extent of 360° divided by the number of blades, symmetrically distributed around the element of consideration. A simple five point average is taken of the wind speed, the five points equally distributed in azimuthal direction at a spacing of ~~20°~~ 30° for the current example with three blades (Figure 8a). Application of this idea to the above highlighted vortex wake simulation yields Figure 8b, which shows an improvement in terms of agreement with the theoretical momentum line for the outboard sections (i.e. the result lie closer to this line). The inboard sections logically experience less inflow velocity variation due to shear and the sector approach appears not to improve the agreement with the theoretical momentum line.

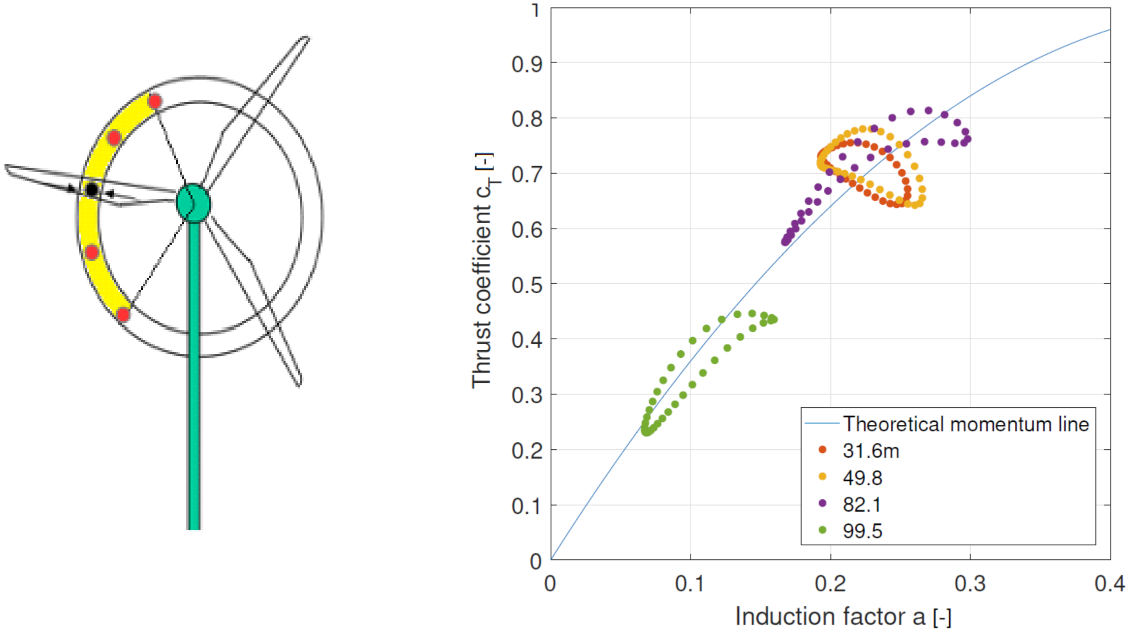

(a) Definition of sector wind for a blade (by averaging over black and red dots), where normally only the black dot is used.

(b) Post-processed AVATAR rotor simulation results in heavy shear (AWSM vortex wake, U=8 m/s, $\alpha = 0.75$) for several radial stations against the theoretical momentum line

Figure 8. ~~Comparison~~ Definition of ~~post-processed AVATAR rotor simulation results in heavy shear (vortex wake, U=8 m/s, $\alpha = 0.75$) for several radial stations against~~ a sector averaged wind and the ~~theoretical momentum line. The~~ effect of using this sector averaged wind speed as reference wind speed for non-dimensionalizing Ct and a~~is now taken as the sector averaged wind speed~~

Implementing the outlined approach in a BEM code has allowed for some further testing in sheared and turbulent inflow as illustrated in Figure 9. In sheared inflow it is shown that induced velocity amplitudes and consequently the normal forces are more in line with the vortex wake modeling. The time trace in turbulent inflow (Figure 9c) clearly illustrates the improved tracking of induced velocity of the sector wind approach, again very close to the vortex wake result except for the higher frequencies. The resulting integrated staircase plots (which are the result of the rainflow counting procedure for obtaining fatigue equivalent loads) show that application of a shed vorticity model (by means of the Beddoes Leishman model ECNAero-BEM-BL instead of the default Snel model for unsteady airfoil aerodynamics) in combination with the sector approach (ECNAero-BEM-BL-sector) results in unsteady loading characteristics matching AWSM very well for this case.

It is recommended to have a more detailed look into the definition of a representative streamtube (e.g. varying azimuthal extent and position leading/lagging, averaging procedure etc.) and run a variety of test cases (e.g. the cases were defined in Table 3 and the parametric shear investigation from Figure 3, containing a variation in the number of blades), also to assure this procedure does not cover up unintentionally other effects such as shed and trailed vorticity variation. Reference is made to a recent publication Madsen et al. (2019) (Madsen et al., 2019) that also addresses the issue of induction tracking by means of a new approach, now solving the BEM equations on a polar grid. This approach seems to resolve the damping of local induced velocities by the dynamic inflow model by decoupling the individual blade momentum equations on a grid. In the current formulation this the momentum equations including dynamic inflow term are solved locally but convergence is assessed by means of the annulus averaged induction (average of the three local axial induced velocities in case of three blades), which inherently introduces a coupling between the elements. This unwanted damping is counteracted by specifying a large number of subiterations per time step to ensure local convergence of the momentum equations (including dynamic inflow term), which is regarded as suboptimal.

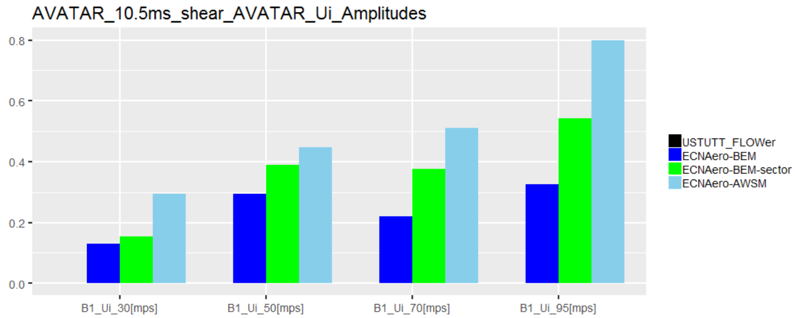

(a) Axial induced velocity amplitudes at 30%R, 50%R, 70%R and 95%R in shear (10.5 m/s)

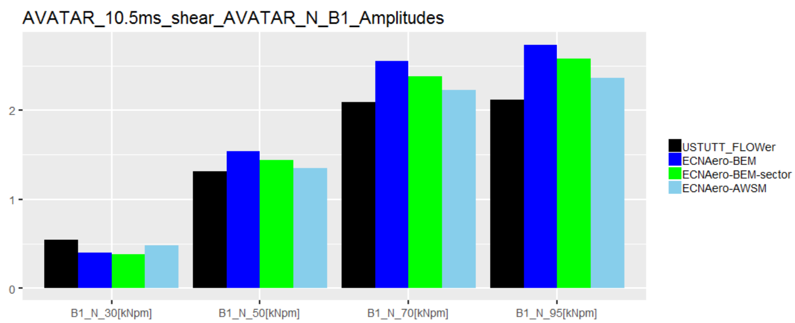

(b) Chordnormal force amplitudes at 30%R, 50%R, 70%R and 95%R in shear (10.5 m/s)

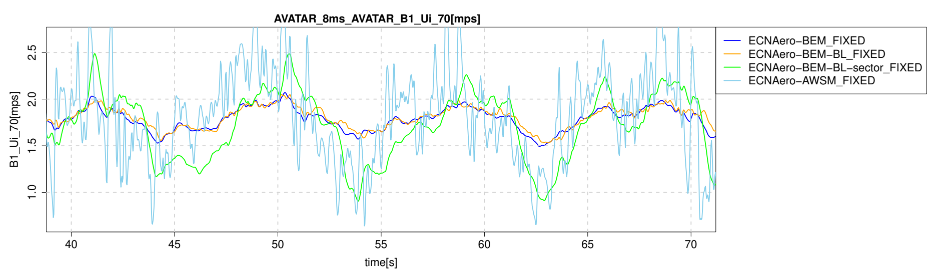

(c) Timetrace of axial induced velocity variation at 70%R in turbulent inflow (8 m/s)

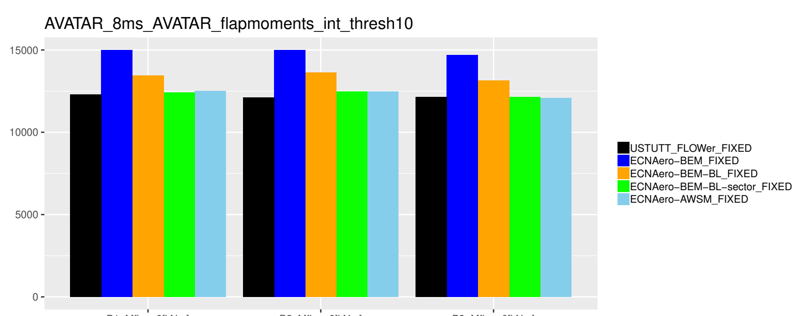

(d) Integrated staircase plot values (above a 10 count threshold) of flapwise blade root moment in turbulent inflow (8 m/s) for all three blades.

Figure 9. Comparison of sector wind BEM implementation (sector) to conventional BEM with Snel and Beddoes Leishman (BL) modeling, vortex wake results (AWSM) and CFD (USTUTT_FLOWer) for selected AVATAR 10MW rotor simulations

3 Validation against field data

Over a decade of measurements on 2.5MW pitch to vane controlled research turbines is available from the EWTW test site Machielse, L.A.H. (2006)(Machielse, L.A.H., 2006). In an attempt to validate fatigue load predictions against field data, these measurements were subject of study.

3.1 Description of set-up

The EWTW farm Eecen et al. (2006) (Eecen et al., 2006) that is subject of investigation consisted of a row of five 2500 kW turbines with variable speed-pitch regulated control. These turbines have a rotor diameter and hub height of 80 m and are placed at mutual distances of 3.8 rotor diameters (D). The farm is very well suited for investigation into effects at full scale because of its state of the art turbines and the comprehensive and reliable measurement infrastructure for turbine and meteorological data.

The farm was orientated from west to east (95-275 °), see Figure 10. Turbine 6 has been instrumented with blade root strain gauges and hence is used for the loads analysis. The wind characteristics are measured with the meteorological tower at 2.5D south-west of turbine 6. This mast measures wind speed and direction at three different heights including hub height. Also air pressure and temperature are measured at this height. More details can be found in the dedicated report Machielse, L.A.H. (2006) (Machielse, L.A.H., 2006). The analyzed measurements at EWTW have been obtained from the period September 2004 until January 2012.

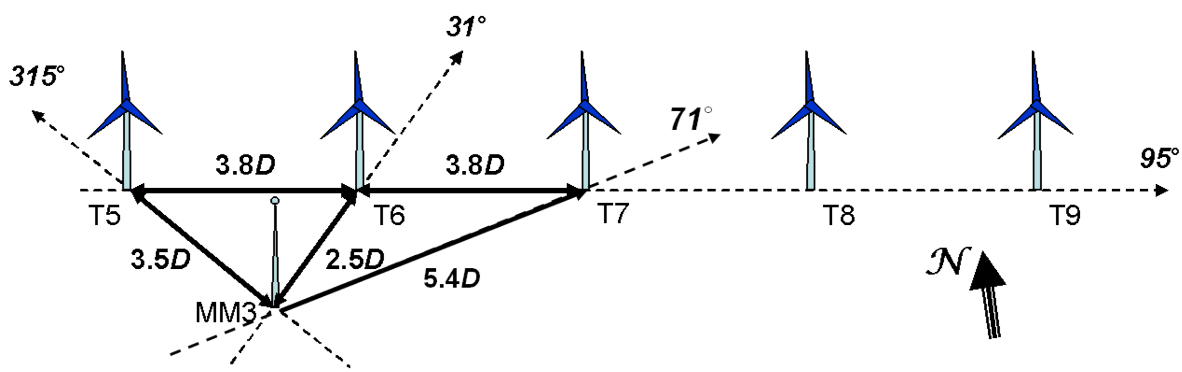

Figure 10. Main dimensions and directions in the EWTW farm. T5 to T9 are the turbine positions, MM3 indicates the measurement mast. Dimensions are expressed in rotor diameters D.

3.2 Data reduction

The SCADA and load signals of turbine 6 together with the meteorological data from mast 3 have been used for the analysis in this report. 10-minute statistics have been retrieved from the data base. A wind direction criterium based on the undisturbed wind sector (between 110-140° and 200-250°) has been applied when retrieving the result from the database, resulting in about 100.000 samples. Further filtering out unwanted conditions (e.g. non-numeric values, start-up, stop or idling conditions) resulted in about 25.000 remaining 10-minute samples. The fatigue equivalent flapwise and edgewise moments of turbine 6 were acquired ~~for for~~ using a slope of 10 for the S-N curve (glass fibre). The rain-flow counting method was applied to the raw signal and the equivalent loads have readily been determined in the database according to IEC 61400-13 ~~iec (2001)~~(iec, 2001). Bin averaging is applied to the resulting data sets both in wind speed and turbulence intensity. The standard error of the mean within each bin is calculated using

$$S = \sigma/\sqrt{N} \quad , \tag{3}$$

with

S	[]	standard error of bin average mean
σ	[]	standard deviation ~~of~~ over the bin data samples
N	[-]	number of samples per bin.

The resulting dataset from the filtering and binning has been visualized using contour plots as a function of turbulence intensity and wind speed, e.g. for the fatigue equivalent flapwise blade root moment in Figure 11a.

3.3 Comparison to simulations

Using the bin averaged operational conditions from the field data analysis, simulations are performed for all wind speed bins (5 to 12 m/s) focusing at the 10% turbulence intensity bin. A full aero-elastic model of the 2.5MW research turbine was built using the PhatAero code as embedded in the FOCUS6 software, including mass, stiffness, control and aerodynamic details as disclosed by the ~~manufacturer.~~ turbine and blade manufacturer. In order to create a representative value for the fatigue loads, six ten minute seeds were created per wind speed bin using the ~~Turbsim wind generator B.J. Jonkman and M.L. Buhl, Jr. (2006)~~ TurbSim wind generator (B.J. Jonkman and M.L. Buhl, Jr., 2006), making sure that the resulting turbulence intensity matched the specification from the field data analysis. Default IEC values were used for shear and turbulence spectra as these details were not available from the measurements. In view of the limited time, the amount of vortex wake simulations (PhatAero-AWSM) was limited to only a few seeds. For each wind speed considered, a representative seed was selected which matched the statistics and equivalent loads compared to the average over the six seeds for each wind speed bin as good as possible. For these specific seeds, the rotational speed variations resulting from the BEM simulations were recorded and fed to the AWSM simulations to have a consistent comparison between them. The settings were similar to the settings as reported in section 2.1.3. The statistics and equivalent loading of all simulation results were obtained after skipping the first 100 seconds, which is regarded as initialisation time, hence using the remaining 500 seconds. Similar to the binning of the measured 10 minute statistics, the simulation results were averaged over the six available seeds for each wind speed bin. In addition to that also the standard error was calculated in accordance with equation 3. To comply with confidentiality requirements, the loads and power have been normalized using the average of the field data results over the wind speed bins. The main comparison plot result is given in Figure 11b. The results for the elected representative seeds are also given indicated by PhatAero-BEM-seeds and PhatAero-AWSM-seeds.

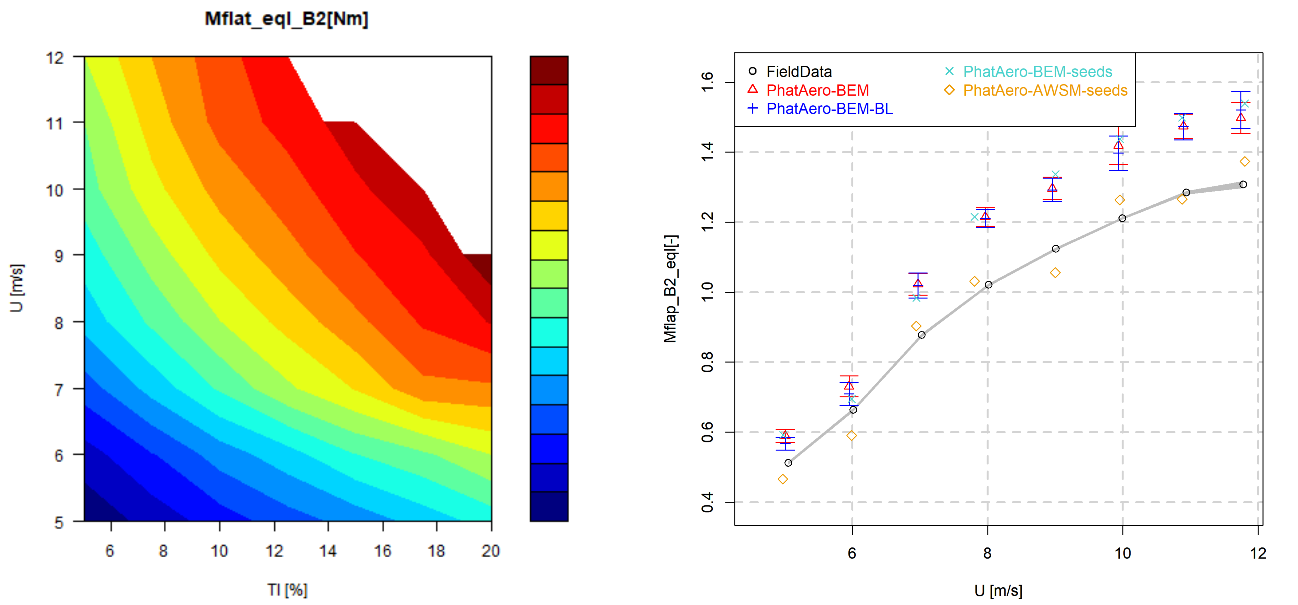

(a) Field data variation with wind speed U and turbulence intensity TI

(b) Comparison between field data and simulations at TI=10% as a function of wind speed (all values are normalized using the average of the field data results over the wind speed bins)

Figure 11. Visualization of damage equivalent flapwise blade root moment

The equivalent loading for the flapwise moments are over predicted around 15% by the BEM simulations (averaged over all seeds and blades), where the AWSM vortex wake simulations are very close to the measurements (-1% averaged over all seeds and blades). A similar conclusion can be drawn for the standard deviation. This trend is similar to the results obtained from the comparison to CFD. Although the absolute difference between measurements and BEM simulations increases with wind speed, the relative difference in terms of percentage remains largely constant over the wind speed range. It is noted that, although not shown here, the averaged flapwise moments are slightly (<5%) underpredicted by the simulations, where they agree well between the different simulation settings.

Application of the Beddoes Leishman model (PhatAero-BEM-BL), which adds modeling of shed vorticity effects, reduces the difference with the measurements only slightly (around 1% decrease). This is not in agreement with the comparison to CFD featuring the 10MW AVATAR rotor, which showed the modeling of shed vorticity to reduce the difference between BEM and high fidelity models significantly. It is unclear at this point what is causing the discrepancy between these observations.

Care should be taken drawing conclusions on the basis of these results, since it is felt that comparing aero-elastic simulations to field data is subject to many uncertainties (inflow, control, model data, compensating errors etc.) that cannot easily be verified. A great effort was made however to eradicate most of these, e.g. by running simulations for a large number of seeds and using a large number of measurement samples. It is recommended to set-up a dedicated field test in an effort to further reduce the underlying uncertainties. Here one can think of using nacelle LiDAR to characterize the inflow conditions in more detail for synthetic wind field creation in combination with unsteady pressure sensors to measure sectional aerodynamic loading. In addition to that it is recommended to include more vortex wake simulations (similar to the number of BEM simulations) to better quantify the difference between these code types. More details about the comparison to field data can be found in the dedicated report Boorsma (2019)(Boorsma, 2019).

4 Impact on IEC design load calculations

Both vortex wake and BEM based models describe the blade aerodynamics on the basis of sectional properties of the airfoils, and both with options to account for dynamic stall effects and corrections for the effects of rotation. This means that the main difference between these model types is the description of the rotor wake aerodynamic effects, which is done in far more detail by the vortex wake methods. Especially for operational conditions with asymmetric and non-uniform rotor loading the more detailed description of the wake influence may give a difference compared with BEM-based wake descriptions. An inventory is made from which conditions and IEC load cases Commission (2009) (Commission, 2009) a difference is to be expected from vortex wake instead of BEM based models. Scoping analyses have been performed with both a BEM and vortex wake code for an entire fatigue load set to verify the differences.

4.1 Conditions and IEC load cases

Load case conditions for which vortex wake descriptions are expected to give more realistic predictions than BEM based models can be categorized as follows. The derivation of BEM theory assumes axi-symmetric (or uniform) inflow conditions with respect to the streamtube considered. Sheared, turbulent or waked inflow conditionsviolate this assumption. As such vortex wake models are expected to provide a more accurate prediction for these conditions. Many BEM based methods have a correction method for by recalling the violations of the underlying BEM assumptions. Here we can mention non-uniform inflow conditions, unsteady disk loading, yaw misalignment, asymmetric blade loads (e.g. pitch steps or coherent wind gusts)that is based on the influence of a cylindrical wake structure with constant wake diameter. For large disk loadings the rotor wake expands, which gives additional non-linear contributions. So especially for high disk loading the dynamic inflow effects are predicted more accurate with vortex wake methods. Most BEM based methods have a correction for the induced velocity distribution in oblique inflow. Most of these corrections are based on empirical fits of the asymmetric disk loading for a few rotors. A more accurate representation of the effects of large yaw misalignment can be obtained with a vortex wake description. Asymmetry between the blade loads can be induced for example by a failed pitch actuator. This cannot be described with most of the BEM based approaches. The effects of large gradients in spanwise circulation are not captured by BEM as there is no radial interaction. Examples are distributed control features actuator failure), spanwise circulation variation (e.g. flaps) or angle of attack reduction towards the tip distributed control, tip effect), radial induction and non-planar blade geometries (e.g. sweep, winglet). For blades with a (nearly-)constant chord and twist towards the blade tip, this effect can be described reasonably well in BEM based codes with the Prandtl tip loss factor. For an arbitrary tip shape (tapered, rounded and reverse

~~twisted)the inflow angle reduction towards the tip can be described well with Vortex Wake methods. Rotors operating at a high disk loading feature wake expansion which is not captured in BEM based models. In cases where the blade has an orientation component perpendicular to the rotor plane (such as large cone angles), radial induction will start to influence blade loads.~~ Although engineering sub-models are developed to overcome most of these limitations, the uncertainties accompanied with these often are large (Boorsma and Schepers, 2018). Eventually it depends on the turbine under consideration (e.g. operating axial induction factor, blade shape), if the load cases listed here give structural loads that are significant for the design. Based on the conditions described here the following load cases from IEC 61400-1 ~~Commission (2009)~~ (Commission, 2009) are considered for evaluation with a vortex wake model.

- Fatigue load cases

  Following the comparison results in this paper, normal power production (DLC1.2) is a candidate for evaluation with a vortex wake model. In general the wake descriptions with vortex wake methods really make a difference if the induced velocities at the rotor are a significant fraction of the ambient wind velocity. This means for example that for a wind near or above the cut-out conditions the wake effects have a very small contribution. Scoping analyses on the production load cases are reported in section 4.2. ~~These load cases contribute to the assessment of the fatigue loads. Both an undetected yaw failure and an undetected individual pitch failure give increased~~ In addition to DLC1.2, operation with failed yaw or failed pitch that is not (yet) detected (DLC2.4) can be considered due to the asymmetric loads over the rotor~~, for which a Vortex Wake description is more detailed.~~

  .

- Extreme load cases

  Prior to analysing some of the ultimate load cases with vortex wake programs, it is recommended to first analyse these load cases with a BEM based program to explore which of the load cases are design-driving. This holds especially for the cases with longer simulation time. Already it is envisaged that ~~for the following load cases~~ DLC1.4 & DLC3.3 ECD (unsteady asymmetric disk loading) and DLC1.5 EWS (non-uniform inflow conditions) calculation with vortex wake models may be more realistic. ~~The direction change gives strong asymmetric loads that are also unsteady. For this condition a vortex wake model is more realistic, while the CPU effort is small for the short time span. Already for the shear of the NWP wind the BEM based calculations give larger blade root bending moment variations than calculations with a vortex wake as was demonstrated in section 2.2. Operation with failed yaw or failed pitch that is not (yet) detected. These load cases contribute to the assessment of the fatigue loads. Both an undetected yaw failure and an undetected individual pitch failure give increased asymmetric loads over the rotor , for which a vortex wake description is more detailed. These cases involve blade failure or yaw failure and may be calculated with a vortex wake method because of the asymmetric rotor disk loading. This is especially the case if e.g. the actuator of one of the blades seizes or has a runaway that eventually triggers the controller to stop by pitching the other blades that do not have pitch failure. Here the direction change gives a strong asymmetric rotor disk loadingwhile the start process itself can be considered as a transient. For this condition a vortex wake program is more realistic, while the time span of the simulation is relatively~~

short. The calculated loads for Although wake effects are anticipated to be small in DLC6 .2 tend to be design driving for some components. For DLC6.2 one usually has to assume that the turbine is not yawing which means that the 50-year EWM may come from many directions and a serious set of calculations may be performed. Besides the fact that DLC6.2 may involve large yaw misalignment the influence of the wake is moderate because of the low rotor disk loading. Here one should realise that for a strong yaw misalignment, one or some of the blades are likely to get in stall which is hard to describe with both a BEM based program and with a vortex wake program. Because of the strong yaw misalignment this load case may be calculated with a vortex wake model. Also here the limitations for both BEM and vortex wake descriptions apply if one or some of the blades get into stall. due to the parked rotor conditions, spanwise circulation variation can still have an impact on the loading.

One may expect that DLC1.3 ETM may be considered for calculation with a vortex wake model because DLC1.3 tends to give design driving loads and because the Extreme Turbulence Model may give highly non-uniform rotor disk loading that is quite unsteady at the same time. Besides the large amount of CPU that is needed for the various 600s calculations one may argue that using a vortex wake model doesn't make much sense because eventually the turbulence level of the EWM has to be scaled such that the extreme blade root bending moments and the largest blade tip deformations match with the 50-year extrapolated values from DLC1.1. This means that if DLC1.3 is calculated with a vortex wake model instead of a BEM-based model, one may end up with a different scaling of the ETM. At least for the blade root bending moments and for the largest tip deformations the use of a Vortex Wake model will not make a serious difference. Differences may be obtained tip displacements this would end up with nearly similar values. However, some differences may appear for the loads in the other turbine components, if the recommended practice of the IEC is followed. wind turbine components.

4.2 Fatigue load set

Scoping analyses have been performed with both BEM based programs and the vortex wake code AWSM for an entire fatigue load set featuring the 10MW AVATAR turbine. Design class IA was used which has a reference wind of 50 m/s, a Weibull average wind of 10 m/s and a characteristic turbulence level of 16%. The wind is modelled with a power law for the vertical shear with exponent 0.2, although for offshore wind turbines the IEC recommendations prescribe a vertical shear exponent of 0.14. The inclination of the ambient wind is set to zero. The wind velocities for which the turbine is in operation range from 4 m/s through 25 m/s while for each wind (with 1 m/s intervals) three calculations are performed with different wind stochastics. For these three calculations the yaw misalignment has values of -8°, +8° and 0°. The turbulence applies to the frequency spectrum of Kaimal and for each wind velocity another random seed was used. In comparison to the rigid rotor calculations which were compared to CFD, the aero-elastic turbine in Phatas was modelled including all flexibilities (e.g. tower and blades) and active controller as defined in the EU AVATAR project. The time increment was set to 0.05s. Simulations were performed with PhatasPhatasSV, Phatas-BSV, PhatAero-BEM and PhatAero-AWSM.

Although the resulting load characteristics were also compared for the tower and nacelle, the results of the flapwise blade root moments are given in Figure 12. This figure shows the largest reductions of the vortex wake model in sub-rated conditions

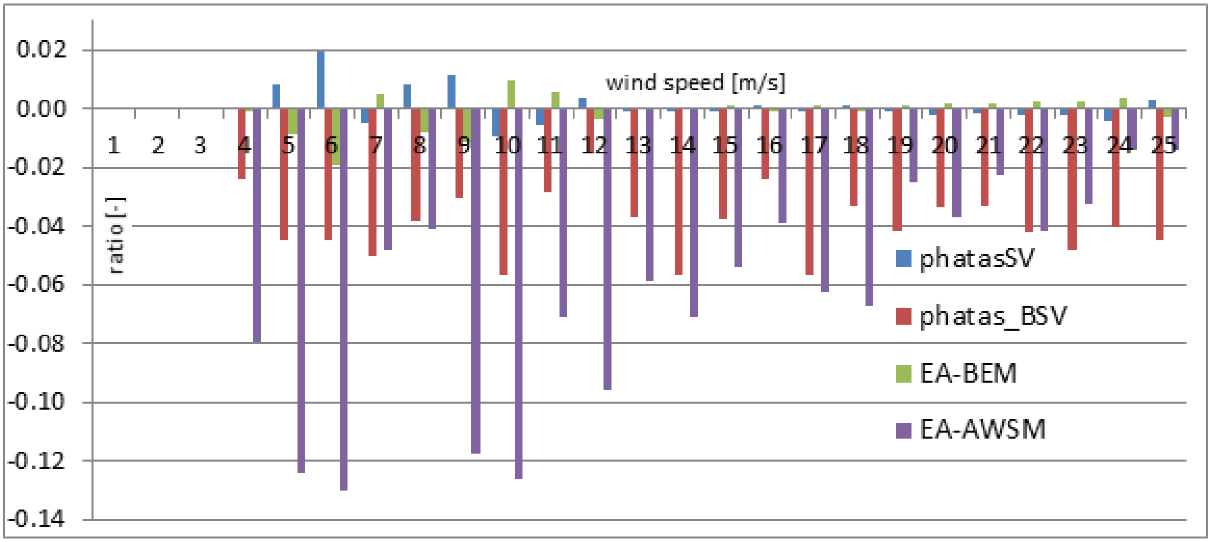

Figure 12. ~~Ratio of blade~~ Blade root flap fatigue loading ratios relative to the average ~~of phatasSV~~ over PhatasSV and PhatAero(EA)-BEM as a function of wind speed

featuring higher axial induction factors, in agreement with the observations from section 2 for the comparison to CFD. For wind velocities above rated the fatigue predictions with blade shed vorticity model (Phatas-BSV) are close to the AWSM vortex wake simulations. The same trends roughly hold for the tower base tilt moment.

Although only a set of normal production load cases is calculated with AWSM it is expected that the reduction in overall fatigue damage by using the program AWSM may be up to 5% for the AVATAR rotor. This is a consequence of the relative large contribution of the higher wind speeds to the overall fatigue. The blade shed vorticity algorithm gives an overall fatigue load reduction of about 2% compared with the BEM based programs without this blade shed vorticity contribution. It is noted that the given percentages are obtained for the AVATAR turbine featuring a low induction rotor and may vary depending on the design operating axial induction. For more details please consult the dedicated report about the IEC load set survey ~~Lindenburg (2019)~~(Lindenburg, 2019).

5 Conclusions

Making a meaningful comparison between CFD ~~(numerical wind tunnel)~~ and lifting line codes has appeared to be quite a challenge in terms of inflow alignment. However a promising engineering approach was devised which allowed successful comparisons in the time domain between these code types. A test matrix was defined covering representative operational and inflow conditions, bearing the CPU requirements in mind. The fatigue load reduction from BEM to vortex wake type codes as observed in the EU AVATAR project has been confirmed by these dedicated CFD simulations. Partly this is explained by the shed vorticity effect which is implicitly included in the vortex wake type codes, but poor tracking of wind variations by induction for BEM remains an issue. It is recommended to further study this aspect to further reduce uncertainties in BEM modeling. In addition to that very similar results were obtained between several vortex ~~type~~ wake codes originating from different institutions. A variety of load cases has shed more light on this subject, showing a correlation of the observations with axial induction factor.

In addition to the comparison against CFD simulations, a validation was made against measured fatigue loads of a real turbine at the EWTW test site. Over 7 years of measurements were analysed to obtain relevant statistics over 100.000 ten minute samples, of which about 25.000 remained after filtering out unwanted conditions. The data was bin averaged with respect to turbulence intensity and wind speed, after which dedicated simulations for each wind speed bin were ran at 10% turbulence intensity. The resulting load comparison shows BEM to over predict the fatigue equivalent flapwise blade root moments, where a vortex wake model comes closer to the measurements. However care should be taken drawing conclusions, since it is felt that comparing aero-elastic simulations to the field data set is subject to many uncertainties (inflow, control, model data, compensating errors etc.) that cannot easily be verified. A great effort was made however to eradicate most of these, e.g. by running simulations for a large number of seeds and using a large number of measurement samples. It is recommended to set-up a dedicated field test in an effort to further reduce these uncertainties, allowing a better validation. Here one can think of using nacelle LiDAR to characterize the inflow conditions in more detail for synthetic wind field creation in combination with pressure sensors to measure sectional aerodynamic loading.

An inventory is made from which conditions and IEC load cases a difference is to be expected from vortex wake instead of BEM based models. Based on past experience it is anticipated that differences are to be expected in non-uniform and yawed inflow conditions especially when operating in high thrust coefficients. Scoping analyses have been performed with both a BEM and vortex wake code for an entire fatigue load set to verify the differences. Although only a set of normal production load cases is calculated with a vortex wake code it is expected that the reduction in overall fatigue damage by using a vortex wake program may be up to 5% for the relatively low induction AVATAR rotor, of which about half was attributed to shed vorticity effects. A more extensive exploration of design load calculations and the added value of vortex wake calculations still is to be performed, not only focusing on fatigue loads but also on extreme loads and power production.

Concluding a very successful validation of lifting line codes against ~~a 'numerical' wind tunnel~~ CFD and field data has been performed. A validation study similar to the cases studied in this project in a physical wind tunnel is recommended as ~~'~~‘proof of the pudding’.

Data availability. Selected simulation data from this paper are available upon request by emailing the corresponding author.

Author contributions. K. Boorsma assembled the simulation results and ran the ECN.TNO simulations. F. Wenz performed all CFD simulations. C. Lindenburg ran the Phatas simulations and performed the survey over the production load set. M. Aman and M. Kloosterman contributed with the Bladed 4.8 simulations.

Competing interests. The authors declare that they have no conflict of interest.

Acknowledgements. This contribution has been ~~sponsored within the framework of TKI Wind op Zee~~financed with Topsector Energiesubsidie from the Dutch Ministry of Economic Affairs.

mede mogelijk gemaakt door
TKI WIND OP ZEE
Topsector Energie

References

IEC TS 61400-13, Wind turbine generator systems Part 13: Measurement of mechanical loads, 2001.

http://www.wmc.eu/focus6.php, 2016.

https://www.3ds.com/products-services/simulia/products/simpack/, 2018.

Bangga, G.: Comparison of blade element method and CFD simulations of a 10 MW wind turbine, Fluids, 3, 2018.

Bangga, G., Lutz, T., Jost, E., and Krämer, E.: CFD studies on rotational augmentation at the inboard sections of a 10 MW wind turbine rotor, Journal of Renewable and Sustainable Energy, 9, 023 304, 2017.

Belessis, M., Chasapogiannis, P., and Voutsinas, S.: Free-wake modelling of rotor aerodynamics: recent developments and future perspectives, in: EWEC 2001, 2001.

B.J. Jonkman and M.L. Buhl, Jr.: TurbSim User's Guide, NREL/TP-500-39797, National Renewable Energy Laboratory, NREL, 2006.

Boorsma, K.: Validation of BEM and Vortex-wake models with full scale on-site measurements, TKI WoZ Vortexloads WP3, Tech. Rep. TNO 2019 R11390, TNO, http://publications.tno.nl/publication/34634925/ZAvbME/TNO-2019-R11390.pdf, 2019.

Boorsma, K. and Schepers, J.: Final report of IEA Task 29, Mexnext (Phase 3), ECN-E-18-003, Energy Research Center of the Netherlands, https://www.ecn.nl/publications/ECN-E--18-003, 2018.

Boorsma, K., Grasso, F., and Holierhoek, J.: Enhanced approach for simulation of rotor aerodynamic loads, Tech. Rep. ECN-M–12-003, ECN, presented at EWEA Offshore 2011, Amsterdam, 29 November 2011 - 1 December 2011, 2011.

Boorsma, K., Chasapogiannis, P., Manolas, D., Stettner, M., and Reijerkerk, M.: AVATAR Deliverable D4.6: Comparison of Aerodynamic Models for Calculation of Fatigue Loads in Turbulent Inflow, http://www.eera-avatar.eu/fileadmin/avatar/user/avatard4.6_v8.pdf, 2016a.

Boorsma, K., Hartvelt, M., and Orsi, L.: Application of the lifting line vortex wake method to dynamic load case simulations, Journal of Physics: Conference Series, 753, 022 030, http://stacks.iop.org/1742-6596/753/i=2/a=022030, 2016b.

Boorsma, K., Greco, L., and Bedon, G.: Rotor wake engineering models for aeroelastic applications, Journal of Physics: Conference Series, 1037, 062 013, http://stacks.iop.org/1742-6596/1037/i=6/a=062013, 2018.

Boorsma, K., Aman, M., and Lindenburg, C.: Improvement of BEM and vortex-wake models, TKI WoZ Vortexloads WP4, Tech. Rep. TNO 2019 R11391, TNO, http://publications.tno.nl/publication/34634926/xeUGvL/TNO-2019-R11391.pdf, 2019a.

Boorsma, K., Aman, M., Lindenburg, C., and Wenz, F.: Validation of BEM and Vortex-wake models with numerical tunnel data, TKI WoZ Vortexloads WP2, Tech. Rep. TNO 2019 R11389, TNO, http://publications.tno.nl/publication/34634924/jVk0uF/TNO-2019-R11389.pdf, 2019b.

Boorsma, K., Wenz, F., Aman, M., Lindenburg, C., and Kloosterman, M.: TKI WoZ VortexLoads Final report, Tech. Rep. TNO 2019 R11388, TNO, http://publications.tno.nl/publication/34634923/tbIASC/TNO-2019-R11388.pdf, 2019c.

Chamorro, L. and Arndt, R.: Non-uniform velocity distribution effect on the Betz–Joukowsky limit, Wind Energy, 16, 279–282, 2013.

Chesshire, G. and Henshaw, W. D.: Composite overlapping meshes for the solution of partial differential equations, Journal of Computational Physics, 90, 1–64, 1990.

Collier, W. and Sanz, J. M.: Comparison of linear and non-linear blade model predictions in Bladed to measurement data from GE 6MW wind turbine, Journal of Physics, 2016.

Commission, I. E.: IEC 61400-3: Design requirements for offshore wind turbines edition 1.0, Tech. rep., IEC, 2009.

Eecen, P. et al.: Measurements at the ECN wind turbine test station Wieringermeer, Tech. Rep. ECN-RX–06-055, ECN, 2006.

Gupta, S.: Development of a Time-Accurate Viscous Lagrangian Vortex Wake Model for Wind Turbine Applications, Ph.D. thesis, University of Maryland, 2006.

Hansen, M. O., Sørensen, N. N., and Michelsen, J.: Extraction of lift, drag and angle of attack from computed 3-D viscous flow around a rotating blade, in: 1997 European Wind Energy Conference, 1997.

Harrison, M., Kloosterman, M., and Urbano, R. B.: Aerodynamic modelling of wind turbine blade loads during extreme deflection events, Journal of Physics: Conference Series, 1037, 062 022, https://iopscience.iop.org/article/10.1088/1742-6596/1037/6/062022, 2018.

Hauptmann et al, S.: Comparison of the lifting-line free vortex wake method and the blade-element momentum theory regarding the simulated loads of multi-mw wind turbines, Journal of Physics: Conference Series, 555, 2014.

Jameson, A., Schmidt, W., and Turkel, E.: Numerical solution of the Euler equations by finite volume methods using Runge Kutta time stepping schemes, in: 14th fluid and plasma dynamics conference, 1981.

Jiang, G.-S. and Shu, C.-W.: Efficient implementation of weighted ENO schemes, Journal of computational physics, 126, 202–228, 1996.

Kim, Y., Lutz, T., Jost, E., Gomez-Iradi, S., Munoz, A., Mendez, B., Lampropoulos, N., N., S., Sørensen, N., Madsen, H., van der Laan, P., Heißelmann, H., Voutsinas, S., and Papadakis, G.: AVATAR Deliverable D2.5: Effects of inflow turbulence on large wind turbines, http://www.eera-avatar.eu/fileadmin/avatar/user/avatar_D2p5_revised_20161231.pdf, 2016.

Kloosterman, M.: Development of the free wake behind a horizontal axis wind turbine, Master's thesis, Delft University of Technology, Delft, the Netherlands, 2009.

Kroll, N., Rossow, C.-C., Becker, K., and Thiele, F.: The MEGAFLOW project, Aerospace Science and Technology, 4, 223–237, 2000.

Leishman, J. and Beddoes, T.: A generalized method for unsteady airfol behaviour and dynamic stall using the indicial method, in: 42nd Annual Forum, American Helicopter Society, Washington D.C., 1986.

Leishman, J. and Beddoes, T.: A semi-empirical model for dynamic stall, Journal of the American Helicopter Society, 34, 3–17, 1989.

Lindenburg, C.: Design load calculations and recommendations for the use of vortex-wake models in the standard, TKI WoZ Vortexloads WP5, Tech. rep., LM Windpower, 2019.

Lindenburg, C. and Schepers, J.: Phatas-IV Aeroelastic Modelling, Release "DEC-1999" and "NOV-2000", Tech. Rep. ECN-CX–00-027, ECN, 2000.

Machielse, L.A.H.: Validatiemetingen EWTW, Eindrapport, Tech. Rep. ECN-E–06-062, ECN, 2006.

Madsen, H., Larsen, T., Pirrung, G., Li, A., and Zahle, F.: Implementation of the Blade Element Momentum Model on a Polar Grid and its Aeroelastic Load Impact, Wind Energy Science, 2019, 53, 2019.

Menter, F. R.: Two-equation eddy-viscosity turbulence models for engineering applications, AIAA journal, 32, 1598–1605, 1994.

Perez-Becker, S., Papi, F., Saverin, J., Marten, D., Bianchini, A., and Paschereit, C.: Is the Blade Element Momentum Theory overestimating Wind Turbine Loads? – A Comparison with a Lifting Line Free Vortex Wake Method, Wind Energy Science, 2019, 70, 2019.

Prandtl, L. and Betz, A.: Vier Abhandlungen zur hydrodynamik und aerodynamik, Göttingen, Germany, 1927.

Schepers, J.: An Engineering Model for Yawed Conditions, Developed on Basis of Wind Tunnel Measurements, Tech. Rep. AIAA-1999-0039, AIAA, 1999.

Schepers, J.: Engineering models in wind energy aerodynamics, development, implementation and analysis using dedicated aerodynamic measurements, Ph.D. thesis, University of Delft, ISBN 978-94-6191-507-8, 2012.

Schepers, J.: Latest results from the EU project AVATAR: Aerodynamic modelling of 10 MW wind turbines, Journal of Physics: Conference Series, 753, 022 017, http://stacks.iop.org/1742-6596/753/i=2/a=022017, 2016.

Schepers, J. and Boorsma, K.: Final report of IEA Task 29, Mexnext (Phase 2), Ecn-e-14-060, Energy Research Center of the Netherlands, https://www.ecn.nl/publications/ECN-E--14-060, 2014.

Schepers, J. and Vermeer, L.: Een Engineering Model voor Scheefstand op Basis van Windtunnelmetingen, Tech. Rep. ECN-CX–98-070, ECN, 1998.

Schulz, C., Fischer, A., Weihing, P., Lutz, T., and Krämer, E.: Evaluation and control of loads on wind turbines under different operating conditions by means of cfd, in: High Performance Computing in Science and Engineering´ 15, pp. 463–478, Springer, 2016.

Shur, M. L., Spalart, P. R., Strelets, M. K., and Travin, A. K.: A hybrid RANS-LES approach with delayed-DES and wall-modelled LES capabilities, International Journal of Heat and Fluid Flow, 29, 1638–1649, 2008.

Snel, H.: Heuristic modelling of dynamic stall characteristics, in: Conference proceedings European Wind Energy Conference, pp. 429–433, Dublin, Ireland, 1997.

Snel, H. and Schepers, J.: JOULE1: Joint investigation of Dynamic Inflow Effects and Implementation of an Engineering Model, Tech. Rep. ECN-C–94-107, ECN, 1994.

Snel, H., Houwink, R., Bosschers, J., Piers, W., Van Bussel, G., and Bruining, A.: Sectional Prediction of 3-D Effects for Stalled Flow on Rotating Blades and Comparison with Measurements, in: Conference proceedings European Wind Energy Conference, Lübeck-Travemünde, Germany, 1993.

Theodorsen, T.: General Theory of Aerodynamic Instability and the Mechanism of Flutter, Tech. Rep. NACA Report 496, NACA, 1935.

Troldborg, N., Sørensen, J. N., Mikkelsen, R., and Sørensen, N. N.: A simple atmospheric boundary layer model applied to large eddy simulations of wind turbine wakes, Wind Energy, 17, 657–669, 2014.

van Garrel, A.: Development of a Wind Turbine Aerodynamics Simulation Module, Tech. Rep. ECN-C–03-079, ECN, 2003.

Wenz, F., Boorsma, K., Bangga, G., Kim, Y., and Lutz, T.: CFD Modelling and Results of VortexLoads WP1, Tech. rep., University of Stuttgart, Institute for Aerodynamics and Gasdynamics, 2019.

Wenz, F., Boorsma, K., and Lutz, T.: Cross-correlation-based approach to align turbulent inflow between CFD and lifting-line-codes in wind turbine simulations, Journal of Physics: Conference Series, To be published in the proceedings of the Science of Making Torque from Wind, Delft 2020, 2020.